Three-Dimensional Numerical Modeling of a Propped Cutter Soil Mix Retention System in Sand

Owen Fraser, *Associate Geotechnical Engineer, JK Geotechnics, Sydney, Australia; email: ofraser@jkgeotechnics.com.au*
Woodie Theunissen, *Principal Associate Geotechnical Engineer, JK Geotechnics, Sydney, Australia, email: wtheunissen@jkgeotechnics.com.au*

ABSTRACT: *The construction of a multi-story building over two basements was proposed adjacent to Botany Bay in Sydney, Australia. The basement excavation required excavations to depths of approximately 6.5 m. The site was surrounded by open parkland on three sides, while on the fourth side a four-story building was present and was offset about 3 m from the site boundary. A tidal creek flowed through a park along the eastern boundary. The site investigation revealed that the subsurface conditions comprised a 16.5 m thick sandy profile overlying a stiff clay layer that in turn overlay better quality interbedded sandy clay and clayey sand. Bedrock was encountered at depths ranging between 21.8 m and 27.32 m. The relative density of sand was initially very loose, but at a depth of about 6 m it quickly increased from loose to dense to very dense. The groundwater table rose to ground level during storm surges and heavy rainfall. Due to the poor relative density of the upper soils and the presence of a high ground water table, a propped Cutter Soil Mix (CSM) wall was selected to support the excavation. To limit ground movements, one row of hydraulic props was installed at the capping beam level and stressed by jacking. One row of props, rather than two, was adopted to overcome constructability issues. This paper presents the geotechnical model used as the basis for the 3D numerical analyses of the shoring system which was completed using PLAXIS 3D. It discusses the refinement of the prop loads and wall stiffness to maintain deflections of the walls to acceptable levels. These results have then been compared with the monitoring data obtained during construction, which includes inclinometer monitoring, survey monitoring of the capping beam, and monitoring of prop loads. The challenges and lessons learned during the design of this shoring system are discussed in this paper.*

KEYWORDS: Numerical analysis, soil-structure interaction, retention system, propped excavation, cutter soil mixing, monitoring

SITE LOCATION: **Geo-Database**

INTRODUCTION

A multi-story residential development over two levels of basement carparking at a site in Dolls Point, Sydney, posed many geotechnical and constructability challenges. An investigation of the site was completed in a staged manner as issues were identified and potential solutions explored. Prior to investigation, it was anticipated that the site would be underlain by deep alluvial deposits with a high water table with sandstone bedrock present at depth. Consequently, the initial investigation of the site comprised the completion of two Cone Penetration Tests (CPT) to better characterize the soil profile and the drilling of four cored boreholes to identify the soils, allow sampling for laboratory testing, determine the depth and quality of the underlying sandstone bedrock, and enable installation of groundwater monitoring wells.

This initial investigation revealed that the key issues facing the site and proposed development were:
- What was the most appropriate means of supporting the structure: piled footings to rock or a raft slab?
- How would the excavation be supported and how would deflections be limited such that the adjoining four-story residential building to the west was not damaged?
- How was the site to be maintained in a dry state during construction?

The depth to rock (up to 27 m) made piling very expensive and a raft slab was considered to be the most economical solution provided feasible. To this end, a further round of investigation comprising Dilatometer (DMT) testing was undertaken, in addition to the previous round of CPT and borehole investigations, to gain a direct measurement of the soil modulus. At the time of the investigation, testing was completed to determine whether a raft slab would be feasible and, consequently, this round of investigation was targeted at the soils below the bulk excavation rather than those above. Whilst sands of good relative density were typically encountered below the basement level, a silty clay layer that varied up to about 2 m thick was encountered at a depth of about 15 m. Analysis showed that compression of this layer under the raft slab loading would result in excessive differential settlement of the slab. Therefore, a piled raft slab was adopted with piles extending below the clay layer and supported on the better-quality soils below. This approach limited differential settlements to the criteria required by the structural engineer. As a Cutter Soil Mix (CSM) wall was proposed to support the excavation, the use of eleven CSM panels (barrettes), installed from the surface and then cut down to below the raft slab, were used in lieu of piles to support the raft slab.

Due to the presence of the adjoining multi-story building supported on a raft slab to the west of the site, care was required that the proposed development would not damage this structure. The high ground water level would have made anchor installation difficult and, although internal propping created some practical difficulties during construction, it was decided that this was the most suitable means of support. However, unlike anchors which are relatively closely spaced and can be stressed to form a fairly uniform force on the wall to limit wall deflections, props are widely spaced for constructability purposes. This means that the retention system must be suitably stiff to span between props without deflecting excessively. It also means that prop loads and prestress jacking forces will vary from prop to prop with each prop interacting with adjoining props. Consequently, prop loads must be carefully specified to achieve a satisfactory outcome. Initially it was proposed to install two rows of props along the western wall to help limit bowing and induced settlement behind the wall. However, due to clashes with the structure, a single row of props installed at the capping beam level was adopted.

While a 3D analysis of the proposed development for the piled raft, retention system, and dewatering of the site was completed, this paper only discusses the analysis and monitoring of the retention system.

CUTTER SOIL MIX WALL

A cutter soil mix wall serves the same purpose as conventional retention systems such as pile walls, but it is constructed in a different manner. The construction process of a CSM wall incorporates cutter wheels mounted on a Kelly bar, as shown in the left frame of Figure 1. As the Kelly bar is lowered into the ground, the cutter wheels remold and mix a binder slurry with the soils to form a panel of improved soil that is rectangular in plan, as shown in the right frame of Figure 1.

Figure 1. Cutter soil mix (CSM) rig and CSM panel.

The benefits of a CSM wall are that it is cost effective, relatively quick to install, relatively impermeable and therefore suitable for use as a groundwater cut-off wall, and the in-situ soil is reused as a construction material (thereby limiting waste). Due to the limitations of the site, a CSM wall was deemed well suited to the conditions present. However, a detailed numerical analysis was required to assess its performance and to ensure the structural design was appropriate.

PROPOSED DEVELOPMENT AND CONSTRAINTS

The proposed residential development comprised a multi-story apartment building over two basement levels. The proposed Bulk Excavation Level (BEL) was RL-4.63mAHD, which accommodates an 800 mm thick piled raft slab, a concrete blinding layer approximately 80 mm thick, and allowance for over-excavation of up to 70 mm. As a result, the basement excavation was expected to extend approximately 6.3 m below existing surface levels. The basement was set back 5.5 m, 5 m, 4 m, and 1.2 m from the northern, southern, eastern, and western boundaries respectively. A neighboring four-story apartment building supported on a raft slab founded on the very loose natural sand was set back between approximately 3 m and 11.2 m from the western site boundary. A tidal creek which flowed directly into the adjacent bay runs just beyond the eastern boundary.

To support the excavation, a 0.64 m thick CSM wall was constructed around the perimeter of the basement which was comprised of six discrete walls. The walls have been designated as Wall 1 to 6 and are shown in Figure 2. CSM walls are formed by mixing binding agents—in this instance, cement—with the aid of water and air within the in-situ soils. To form the wall, a series of interlocking 2.8 m long by 0.64 m thick panels were constructed. Each new panel was cut into the panel beside it to form a continuous "watertight" wall. While the cement/soil mix was still wet, vertical steel beams were inserted into the CSM wall to increase the wall stiffness and tensile capacity. The CSM wall was supported by a single row of eleven props installed at the level of the capping beam (RL1.15mAHD) that were then jacked to various magnitudes to limit wall movements. The props have been designated S1 to S11 and are also shown in Figure 2. The piled raft slab was connected to the CSM wall; staged modeling of the loads applied to the raft slab was required to model the interaction between these elements. The schematic view of the 3D numerical model is presented in Figure 2, which includes the piled raft slab, CSM wall, props, and applied surcharge loads.
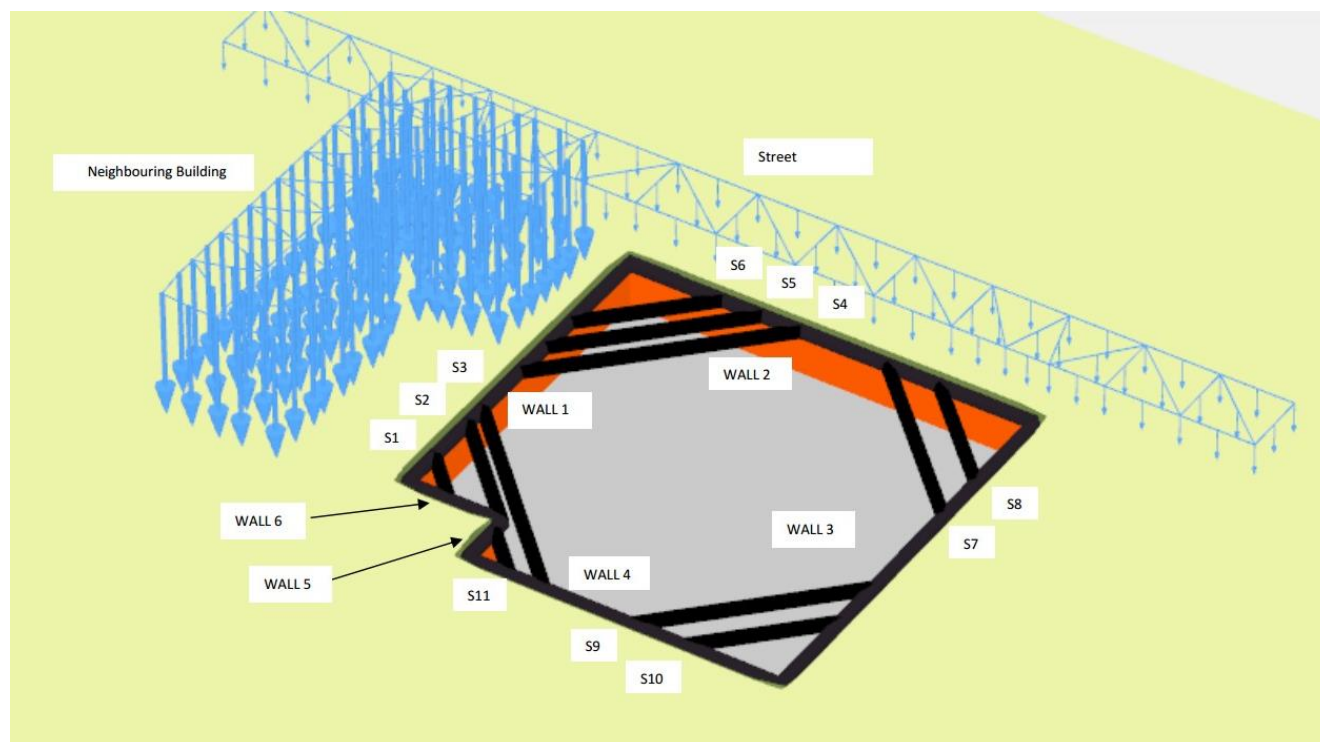

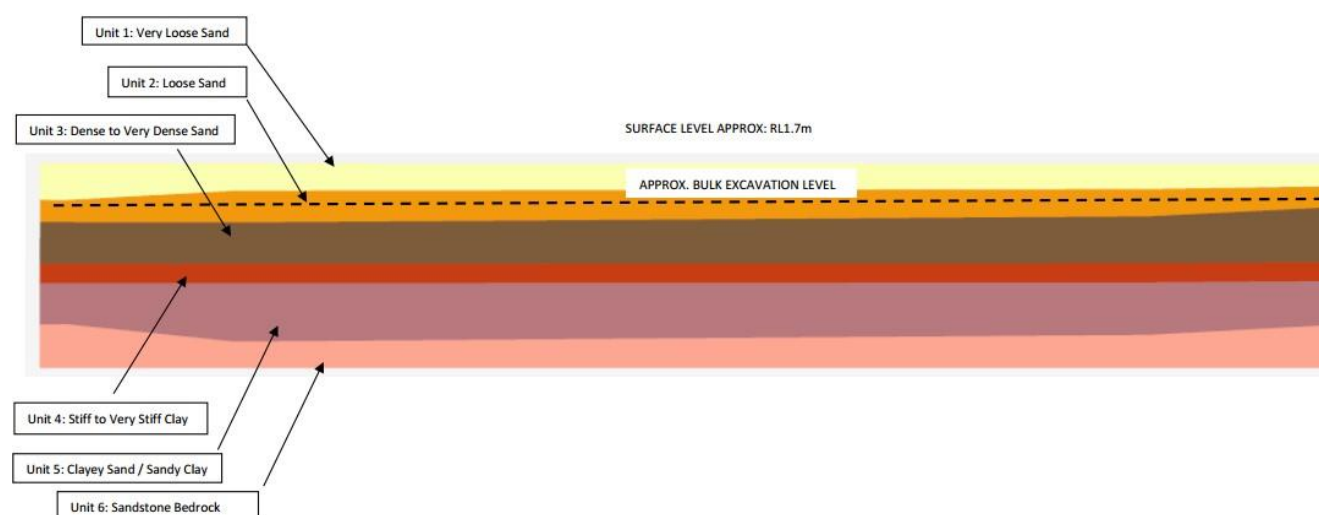*Figure 2. Screenshot of the three-dimensional model using the software Plaxis 3D.*

NUMERICAL MODEL

A three-dimensional model of the site, the proposed development, and boundary conditions was generated using the computer software Plaxis 3D. This model was developed using the provided survey data and the geotechnical information obtained from the geotechnical investigations. The geotechnical model is discussed further below.

Geotechnical Model

The subsurface profile generally included sand that was initially of very loose relative density, improving to loose relative density between approximately 3.4 m to 5.5 m depth below surface levels, i.e., about 2.9 m to 0.8 m above the bulk excavation level. Below this the relative density of the sand quickly increased to medium dense and dense with dense to very dense sand, encountered at about 11.7 m and deeper. The sand overlay stiff to very stiff strength silty clay at between approximately 14.5 m and 15.8 m depth, which in turn overlay interbedded clayey sand and sandy clay with sandstone bedrock, encountered at depths of about 21.8 m to 27.32 m below existing surface level.

The depth of the soil units varied across the site but were relatively horizontal given the size of the site and the depositional nature of the marine sands. Given the shallow depth of the fill, which was typically less than 0.7 m, and the similarity of its material properties to the upper very loose sand, the fill was not individually defined in the model but was included as part of the upper very loose sand unit. This simplification of the model was adopted due to numerical difficulties that may be experienced when modeling thin layers. A cross-section of the subsurface profile is presented in Figure 3.

Figure 3. Generalized section of subsurface profile used in the 3D model.

Key to the successful modeling of the performance of the proposed retaining wall was the selection of representative material parameters, particularly the modulus values of the soils. Geotechnical parameters were selected for each geological unit based on the completed in-situ testing, which comprised boreholes with Standard Penetration Tests (SPT), CPT, and DMT. The SPT, CPT, and DMT data was then interpreted using empirical correlations well established in geotechnical engineering (*Denver 1982, Bowles 1988, Poulos 1988, and Marchetti et al. 2001*).

When the calculated modulus values were compared, the results suggested that the variability in stiffness with depth was typically horizontal with little variation across the site, although the modulus values calculated using established relationships from the SPT "N" values were significantly lower than those calculated from either the CPT or DMT test results. The calculated CPT and DMT modulus values correlated fairly well, but overall the CPT values were lower than the DMT modulus values. This can be seen below in Figures 4 and 5. The DMT results, being a direct measurement of the modulus of the material, were considered most representative of the modulus of the material, with the CPT values providing confidence that ground conditions across the site were fairly consistent.
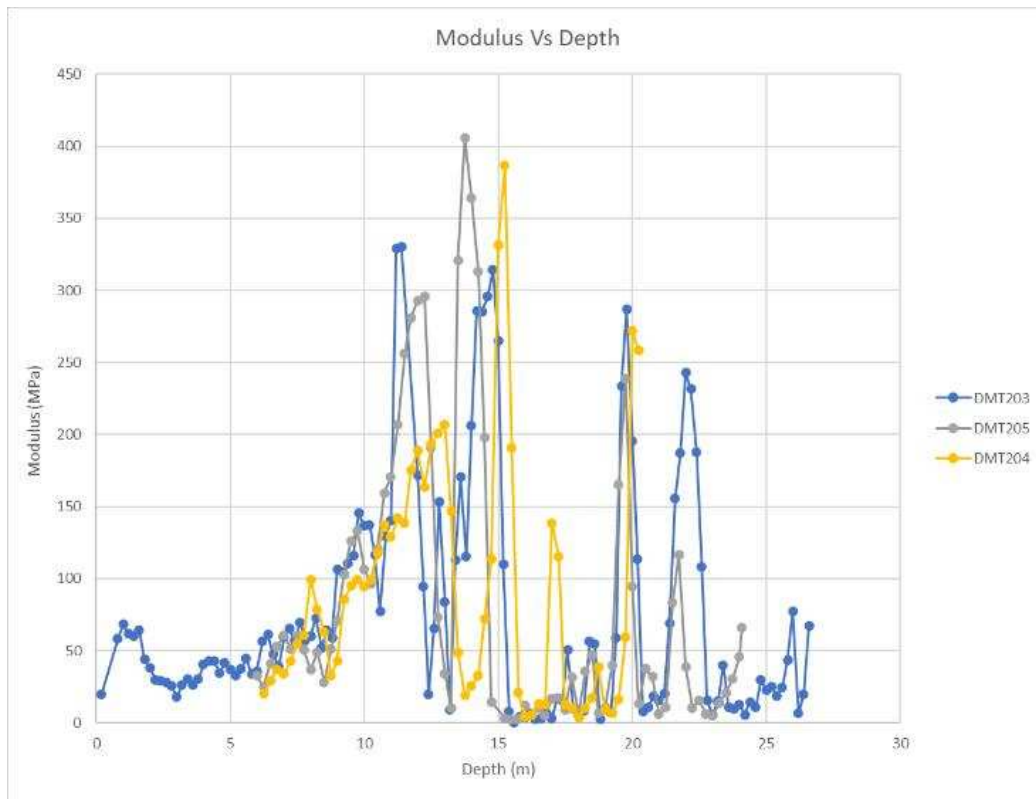
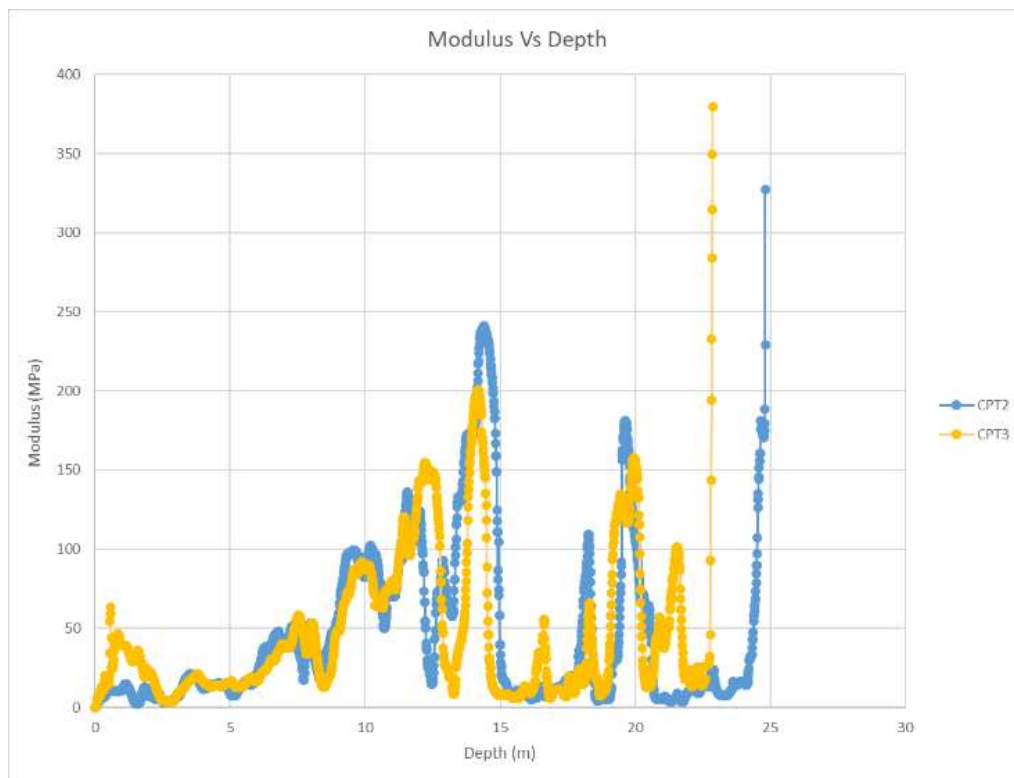*Figure 4. Calculated modulus values from DMT results.*

Figure 5. Calculated modulus values from CPT results.

The soils were modeled using the Hardening Soil model with small strain stiffness (HSS) (*Schanz et al. 2000)*. In our selection of these parameters, consideration was given to the inherent uncertainty associated with natural, non-engineered materials, such as variability in relative densities/strength, modulus, and permeability. The adopted parameters in the numerical model are presented in Tables 1 and 2.

Table 1. Hardening Soils Small Strain Material Parameters.

Material	Saturated Unit Weight (kN/m³)	Unsaturated Unit Weight (kN/m³)	Cohesion (kPa)	Internal Angle of Friction (deg)	Dilation Angle (deg)
Very Loose Sand	17	15	0	28	0
Loose Sand	18	16	0	30	0
Dense to Very Dense Sand	22	20	0	36	6
Stiff to Very Stiff Clay	19	17	2	28	0
Clayey Sand/Sandy Clay	20	18	0	33	3

Table 2. Hardening Soils Small Strain Modulus Parameters.

Material	Secant Stiffness E_{50} (MPa)	Tangent Stiffness E_{oed} (MPa)	Unloading/ Reloading Stiffness E_{ur} (MPa)	Reference Shear Modulus G_o (MPa)	Shear Strain at $0.7G_o$
Very Loose Sand	20	20	60	62.5	1.5×10^{-4}
Loose Sand	50	50	150	156.3	1.5×10^{-4}
Dense to Very Dense Sand	161	161	483	503	1.5×10^{-4}
Stiff to Very Stiff Clay	8.4	4.2	25.2	26.25	1.5×10^{-4}
Clayey Sand/Sandy Clay	50	50	150	156.3	1.5×10^{-4}

Interaction reduction factors (R_{inter}) of 0.9 and 0.67 were adopted for the sandy and clayey soils, respectively. This factor relates the interface strength (wall friction and adhesion) to the soil strength (friction angle and cohesion) and models the reduction in shear strength between the two dissimilar materials. The adopted rate of stress dependency in the stiffness behavior "m" was 0.5 and 1.0 for sand and clay, respectively.

The groundwater level was measured between RL0.4mAHD and RL1.0mAHD; for the purposes of the model, a uniform groundwater level at RL0.7mAHD was assumed, although sensitivity testing was completed with the groundwater table modeled at the surface. Existing surface levels varied from between about RL1.3mAHD to RL1.6mAHD.

Structural Model

Following the deletion of the second row of props (i.e., only one row of props was installed at the capping beam level) and to limit deflection of the western wall (Wall 1) and thus the potential impact on the adjoining building to the west, additional steel reinforcement was placed in this wall. Due to variations in the geometry of the capping beam and differing spacing of the vertical steel beams installed into the CSM walls, the structural parameters varied between walls. Furthermore, the vertical and horizontal stiffness differed for the CSM wall, as reinforcement comprised only vertical steel beams. Consequently, a higher modulus was adopted for the vertical than the horizontal direction. The adopted structural parameters are summarized in Tables 3 and 4.

The CSM wall, the capping beam and raft slabs (which includes the neighboring building's raft slab) were modeled as continuous plate elements with interface elements on both sides to model the wall/raft to soil interaction. The piled raft slab and CSM wall connection was modeled as pinned/flexible, and therefore shear and axial forces were able to be transferred at the connection but bending moments were not. The props were modeled as node-to-node anchors with a prestress applied at the relevant modeling stage.

The CSM walls were 19.3 m deep and extended approximately 13.2 m below the bulk excavation level with the wall toe at RL-17.9mAHD. The wall depth was not governed by stability considerations but was instead dictated by the necessity to form a groundwater cut-off within the low permeability clays that were present at depth. The purpose of the cut-off wall was to control the groundwater inflow into the basement during construction. In the long term, the basement was constructed as a tanked structure.

Table 3. Structural Parameters Adopted – Plate Elements.

Structural Element	Bulk Unit Weight*	Young's Modulus (MPa)**	Thickness/Plan Dimensions (mm)	Poisson's Ratio
Cutter Soil Mix Wall – Wall 1				
Temporary Case	17	10,600 / 1,060	640	0.135
Permanent Case	17	7,500 / 750	640	0.135
Cutter Soil Mix Wall – Walls 2 to 6				
Temporary Case	17	10,000 / 1,000	640	0.135
Permanent Case	17	6,910 / 691	640	0.135
Capping Beam – Wall 1	24	20,880	900 to 1,070	0.15
Capping Beam – Walls 2 to 6	24	19,200	900	0.15
Raft Slab	24	19,200	800	0.15
Neighboring Building – Raft Slab	0***	19,200	150	0.15

* As plates are superimposed on a continuum and therefore "overlap" the soil, the unit weight of the soil has been subtracted from the unit weight of the plate; however, Table 3 presents the actual unit weight of the element.
** To model the difference in the vertical and horizontal stiffness of the CSM walls, the higher modulus value was assigned to the vertical direction (z axis) and the lower modulus value was assigned to the horizontal direction (x and y axes).
*** The weight of the raft slab was included in the uniformly distributed loads applied in the model.

Table 4. Structural Parameters Adopted – Props.

Structural Element	Young's Modulus (MPa)	Area (m²)
MP150 Props	200,000	0.02203
MP250 Props	200,000	0.02346
Super MP250 Props	200,000	0.0605196

Prop Details

The prop numbers, prop type, span, and prestress details applied at installation (Stage 4) are presented in Table 5. For the locations of the props, reference should be made to Figure 2.

In the numerical model, all props were prestressed simultaneously, although it should be noted that two props, S3 and S9, were not stressed and were passive. As the load on one prop affects the force in adjoining props and the long-term deflection of the wall, it was important that this assumption was replicated as closely as possible during construction.

Table 5. Prop Details.

Prop Number	Prop Type	Span (m)	Prestress Applied at Installation (kN)
S1	MP150	5	490
S2	MP150	13	700
S3	Super MP250	25	0
S4	Super MP250	25	50
S5	MP250	19	850
S6	MP250	13	900
S7	Super MP250	21	250
S8	MP250	13	1,800
S9	Super MP250	21	0
S10	MP250	13	1,750
S11	MP150	5	350

Applied Loads

The details of the applied loads in the numerical model are summarized below.

- The raft slab loads were applied at the column and wall locations, and generally varied between line loads of 23 kN and 910 kN per meter for the walls and between 2,150 kN and 5,500 kN for the columns. A line load of 300 kN per meter was applied to the top of the CSM walls. These loads were provided by the structural engineer and are unfactored (i.e., serviceability) loads.

- Construction loads were applied as uniformly distributed loads (UDL) at various modeling stages and ranged from 5 kPa to 20 kPa. Consideration was also given to the temporary setup of mobile cranes which were modeled by the application of a 50 kPa UDL.

- For the neighboring building, a 40 kPa UDL was adopted over the whole slab area.

- For the adjacent roadway, a 10 kPa UDL was adopted.

For the neighboring building, the footing system was determined to be a stiffened raft slab, although the as built dimensions and load distribution on the slab could not be accurately determined. As a result, the design loading was simplified to a UDL applied over the full surface of the slab. Whilst it is true that this approach oversimplifies the interaction between the raft slab and soils, it was assessed to be appropriate for modeling purposes. This assessment was made by comparing the difference in performance for both the building and retention system when an equivalent discrete strip footing load was modeled and compared with the impact of a UDL. The results of this assessment indicated that while an applied UDL has a greater impact on the retaining wall than discrete strip loads, the impact on the adjoining building was that larger settlements were induced where a discrete strip load was modeled. However, in the absence of information on actual slab dimensions and loadings and considering the marginal difference in both the impact on the retention system and induced settlements below the adjoining building, the adoption of a UDL was considered an appropriate approach.

Model Staging

The adopted stages to model the existing conditions and the construction procedure were as follows:

1. Begin initial phase to generate the initial stress state;

2. Consider existing conditions: apply adjacent roadway, neighboring building, and construction surcharge loads;

3. Install the CSM wall and capping beam, and commence site dewatering;

4. Dewater and excavate to RL0.15m, and install and prestress the props at RL1.15m;

5. Dewater and excavate to BEL of RL-4.7m (construction loads were changed at this stage);

6. Construct the concrete blinding layer at BEL;

7. Construct the raft slab;

8. Apply 20% of the total column loads;

9. Install the basement Level 1 floor slab (construction loads were changed at this stage);

10. Apply 40% of the total column loads;

11. Remove the temporary props;

12. Install the ground floor slab;

13. Apply 100% of the total column loads;

14. Place fill to raise site levels; and

15. Cease site dewatering.

Model displacements were reset to zero at the start of Stage 3, as this allowed for an assessment of only those displacements associated with the construction.

DESIGN PROCESS

Despite the computing power and specialized software currently available that allows for the completion of a detailed numerical analysis, the process contains a number of inherent risks that must be mitigated during the design process. These risks are:

- The appropriate characterization of the subsurface conditions and the inherent variability that exists;

- The appropriate representation of the proposed structure, which includes the geometry, material parameters, and the soil-structure interaction;

- The realistic and accurate sequencing of the construction staging;

- The accurate input of data and understanding of the limitations of the software and constitutive model; and

- Poor or incomplete communication between the various parties involved, both in the design and construction of the project.

To manage the above risks, the following considerations are required during the design stage:

- All input data to be carefully checked, not just by the modeler but also the reviewer. This must include:

  o A check of the model that forms the basis of the numerical model as well as assumptions that have been made in the formulation of this model;

  o The input data, including the geometry, material parameters, elements used to represent physical features (and their limitations), and the construction sequencing; and,

o Some simple hand calculation checks.

- In addition to a check of the input data, a sensitivity analysis must also be completed to gain an understanding of the physical implications of any assumptions made. If this analysis indicates that significant ramifications may result if the assumptions or approximations are incorrect, then either further proving will be required to confirm these assumptions/approximations or a conservative risk averse approach must be adopted. Where a conservative approach is adopted, the client must be made aware of the cost/space implications of such an approach.

- Where risks are identified and all parties are fully informed of these risks and their implications, potential mitigation measures must be devised and be ready to be implemented should pre-set criteria be exceeded during construction. The cost and time implications and potential reputational damage associated with implementing these remedial measures should be considered.

- As the soil-structure interaction encompasses the domains of two different disciplines—geotechnical and structural engineering—clear and effective communication between the geotechnical and structural engineers is essential in the completion of successful analysis and design. Both disciplines must work closely together in a collaborative manner. Similarly, the builder (if possible) should be included in the design process so that the analysis faithfully represents the proposed construction staging.

During construction, an observation of the performance of the structure and surrounding materials or structures is required to provide a feedback loop. This is mandatory at key stages during construction and is necessary to allow the model to be checked to confirm whether it has reliably predicted the performance that is being observed in the field. If the model has not accurately predicted the performance, it allows the model to be recalibrated and if design criteria are (or will be) exceeded at later stages in construction, it allows for remedial measures to be initiated. This feedback loop may include information obtained from load testing of piles, survey monitoring, the results of inclinometer or extensometer monitoring, etc.
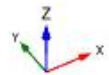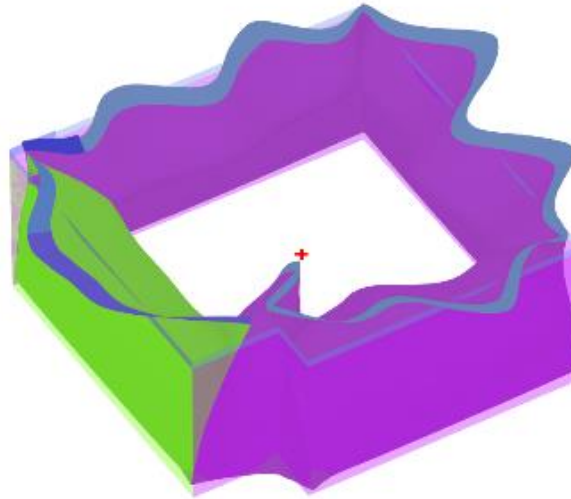
NUMERICAL ANALYSIS RESULTS

Predicted CSM Wall Lateral Displacements and Prop Forces

Table 6 summarizes the lateral displacements of the CSM walls predicted at various stages based on the numerical model. While predictions were provided for all walls, only the predictions for Walls 1, 2, and 3 have been presented, which were the walls that were monitored during construction. Positive displacements reflect displacements into the basement excavation, while negative values indicate movements back into the retained soil. Reference should be made to Figure 6, which presents the heat map indicating the predicted total (horizontal and vertical) displacements for Wall 1 at Stage 13 where 100% of the column loads have been applied.
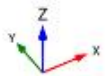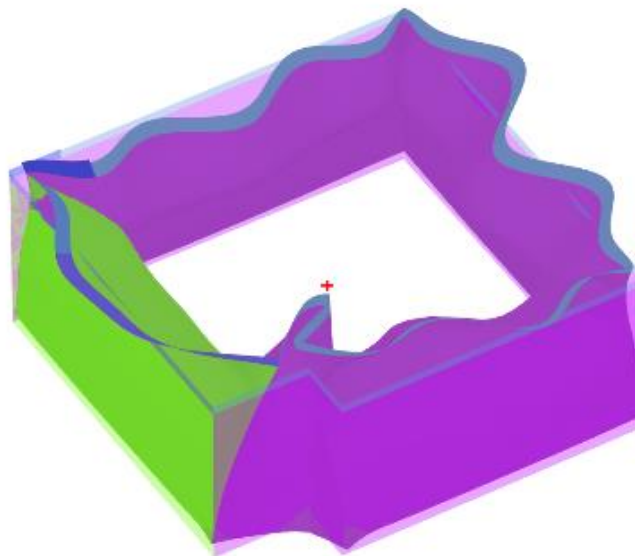
Table 6. Predicted CSM Wall Lateral Displacements.

CSM Wall	Stage 4 Installation of Props and Walers	Stage 5 BEL to RL-4.7m	Stage 8 20% Load on Raft Slab	Stage 10 40% Load on Raft Slab	Stage 13 100% Load on Raft Slab
Wall 1	Min = -9.5mm Max = 0.9mm	Min = -13.2mm Max = 14.7mm	Min = -12.9 mm Max = 15.0mm	Min = -12.8mm Max = 15.1mm	Min = -6.8mm Max = 15.1mm
Wall 2	Min = -9.4mm Max = 0.8mm	Min = -6.1mm Max = 18.6mm	Min = -6.0mm Max = 18.8mm	Min = -5.9mm Max = 18.8mm	Min = -0.3mm Max = 19.0mm
Wall 3	Min = -14.0mm Max = 0.9mm	Min = -17.6mm Max = 14.6mm	Min = -17.4mm Max = 14.8mm	Min = -17.3mm Max = 14.8mm	Min = -10.8mm Max = 14.7mm

Table 6 provides an overview of the predicted lateral displacements, while Figure 6 graphically indicates vector displacements of the CSM walls. This shows that displacements are primarily lateral, with relatively minor vertical displacements (settlement) occurring. Furthermore, evidently the majority of the displacements occur at two stages: at bulk excavation (Stage 5) and following the destressing and removal of the props (Stage 13).

Total displacements |u| (scaled up 500 times)

Maximum value = 0.02309 m (Element 1385 at Node 1206)

Total displacements |u| (scaled up 500 times)

Maximum value = 0.02331 m (Element 1402 at Node 22359)

Figure 6. Comparison of the CSM wall displacements before and after removal of the props.

Due to the flexibility of the CSM wall, the stressing of the props results in sections of the wall undergoing displacement away from the basement excavation and into the retained soil. However, between the prop locations and primarily at the center of the walls, the walls generally undergo displacement into the excavation. Following the removal of the props, the walls relax and undergo displacement into the excavation despite the presence of the floor slabs providing lateral support. Figure 6 compares the wall movements between Stages 10 and 13 (i.e., before and after the removal of the props), where the green wall denotes the western wall (Wall 1). Displacements are exaggerated by 500 times. This shows that despite the rigidity of the walls and concrete floor slabs, appreciable movements occur once the props are removed.

The predicted prop forces are presented below in Table 7.

Table 7. Predicted Prop Forces (kN).

Prop	Stage 5 BEL to RL-4.7m	Stage 8 20% Load on Raft Slab	Stage 10 40% Load on Raft Slab
S1	1170	1093	1100
S2	1131	1180	1197
S3	1009	911	936
S4	1036	1098	1134
S5	1191	1193	1207
S6	1717	1731	1744
S7	1453	1511	1554
S8	2168	2192	2207
S9	1247	1282	1310
S10	2191	2224	2242
S11	1133	938	940

Predicted Displacements Below the Neighboring Building

As a result of the proposed development, displacements were induced below the neighboring building. Based on the analysis, it was anticipated that maximum settlements would be in the order of 17 mm. While just over three quarters of these induced settlements resulted from the deflection of the retention system, the remaining settlement was associated with the settlement bowl induced by the loading of the piled raft slab. This can be seen below in Figure 7, which shows the predicted settlements induced below the adjoining building.

The induced displacements below the adjoining building were a key consideration in the design of the CSM wall and the props, including the prop prestress. The structural engineer carried out the assessment of the acceptable displacements of the floor slab.

CONSTRUCTION MONITORING

To provide confidence in the accuracy of the modeling, a monitoring program was carried out during construction with the following details:

- The monitoring of five inclinometers installed to depths varying between 14 m and 15 m. Inclinometers 101, 102, and 103 were installed in CSM Wall 1 on the western boundary; Inclinometer 104 was installed in CSM Wall 2 on the northern boundary; and Inclinometer 105 was installed in CSM Wall 3 on the eastern boundary. Monitoring was carried out at critical construction milestones over about 7 months.

- The installation of four survey monitoring points on the capping beam: three were installed on CSM Wall 1 and one was installed on CSM Wall 3.

- The real-time monitoring of prop forces in props, S3, S4, and S8.

Monitoring during construction targeted CSM Wall 1, which runs along the western boundary. Movements along this boundary were of primary concern due to the presence of the four-story apartment building supported on a raft slab in the adjoining property. Monitoring of CSM Wall 3 along the eastern boundary was also completed due to the presence of the adjacent drainage channel. No movement sensitive structures were located along the remaining two boundaries.
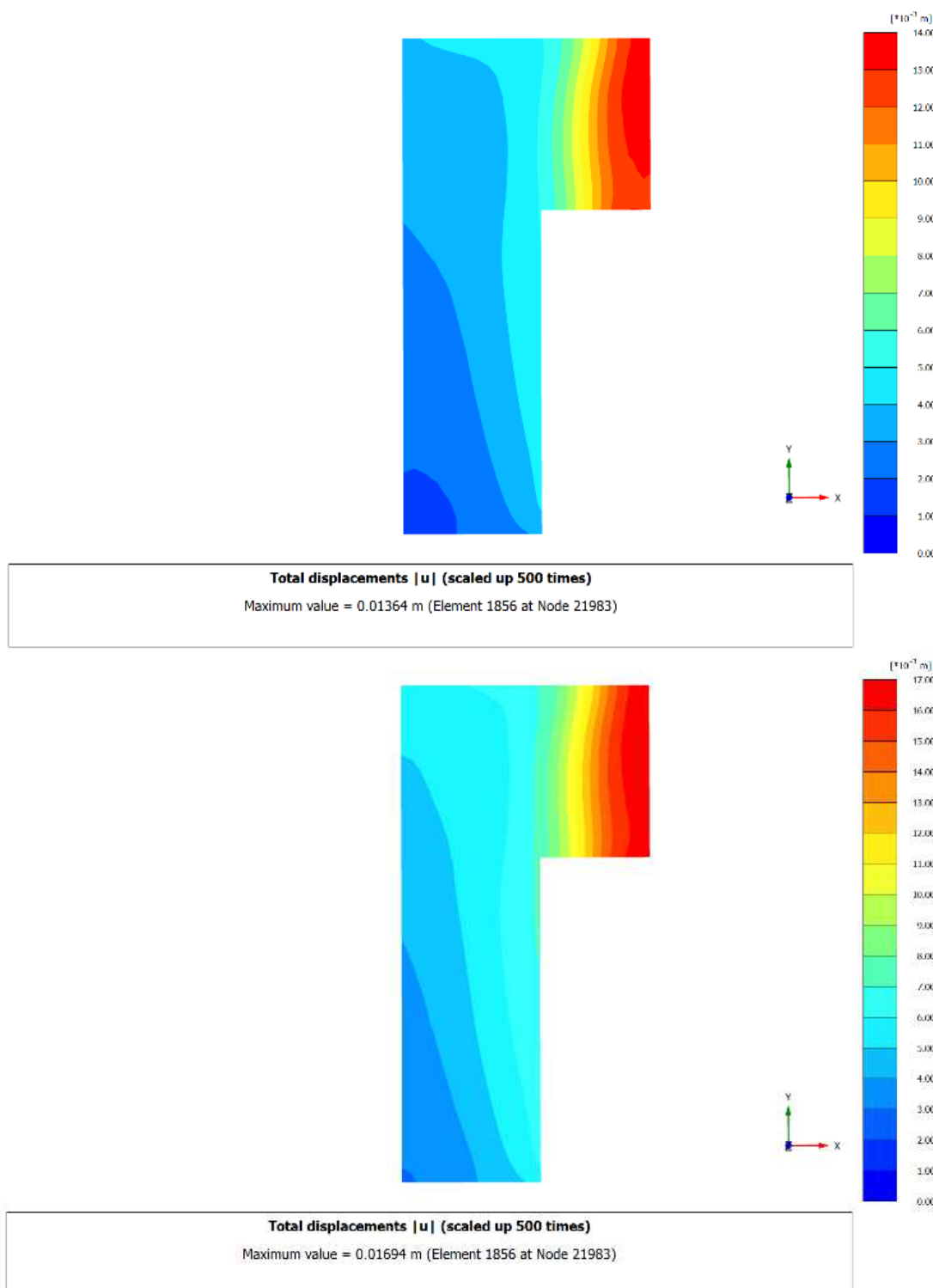

Total displacements |u| (scaled up 500 times)
Maximum value = 0.01364 m (Element 1856 at Node 21983)

Total displacements |u| (scaled up 500 times)
Maximum value = 0.01694 m (Element 1856 at Node 21983)

Figure 7. Comparison of total displacement below the neighboring building slab following the removal of props (11) and the completion of construction (Stage 15).

COMPARISON OF MONITORING RESULTS WITH PREDICTED MOVEMENTS AND FORCES

Introduction

Inclinometer and survey monitoring was completed at critical stages during construction at five locations (Figure 8). This monitoring was completed to provide feedback on the suitability of the design assumptions made and the accuracy of the numerical modeling predictions and was completed during construction. This is an important feedback loop and risk management strategy; it allows for early intervention prior to damage to adjoining movement sensitive structures or catastrophic collapse.

Figure 8. Inclinometer locations.

Inclinometer Monitoring

The inclinometers casings were installed in the CSM walls by fastening them to the steel I beams that were inserted in each constructed panels. These I beams did not extend to the toe of the wall. Consequently, while the toe of the wall was formed at RL-17.9m, approximately 19.3 m below existing ground level, the inclinometers, with the exception of Inclinometer 104, extended to a depth of 15 m (i.e., about 4.3 m above the toe of the wall). Inclinometer 104 was installed to a depth of 14 m (i.e., about 5.3 m above the toe of the wall). Based on the results of the numerical modeling, the inward movement and rotation of the wall were predicted to occur at the toe of the wall. At the base of the inclinometers, horizontal movement was anticipated to range from 1.2 mm to 1.8 mm. Rotation was predicted to be about 0.004°, which results in less than 1 mm of deflection at the top of the inclinometer.

The results of the inclinometer measurements at each of the five locations are provided below in Figures 9 to 13.

However, as the inclinometer casing did not extend to the toe of the wall and was not fixed in space, the inclinometers failed to capture between 1.2 mm and 2 mm of movement, and thus underestimated the total displacements. Consequently, based on the predicted movements at the toe of each of the inclinometers, the inclinometer results were adjusted to provide a more accurate representation of the wall movements. The measured inclinometer results, adjusted inclinometer results, and predicted movements at each of the inclinometers are shown in Figures 14 to 18.
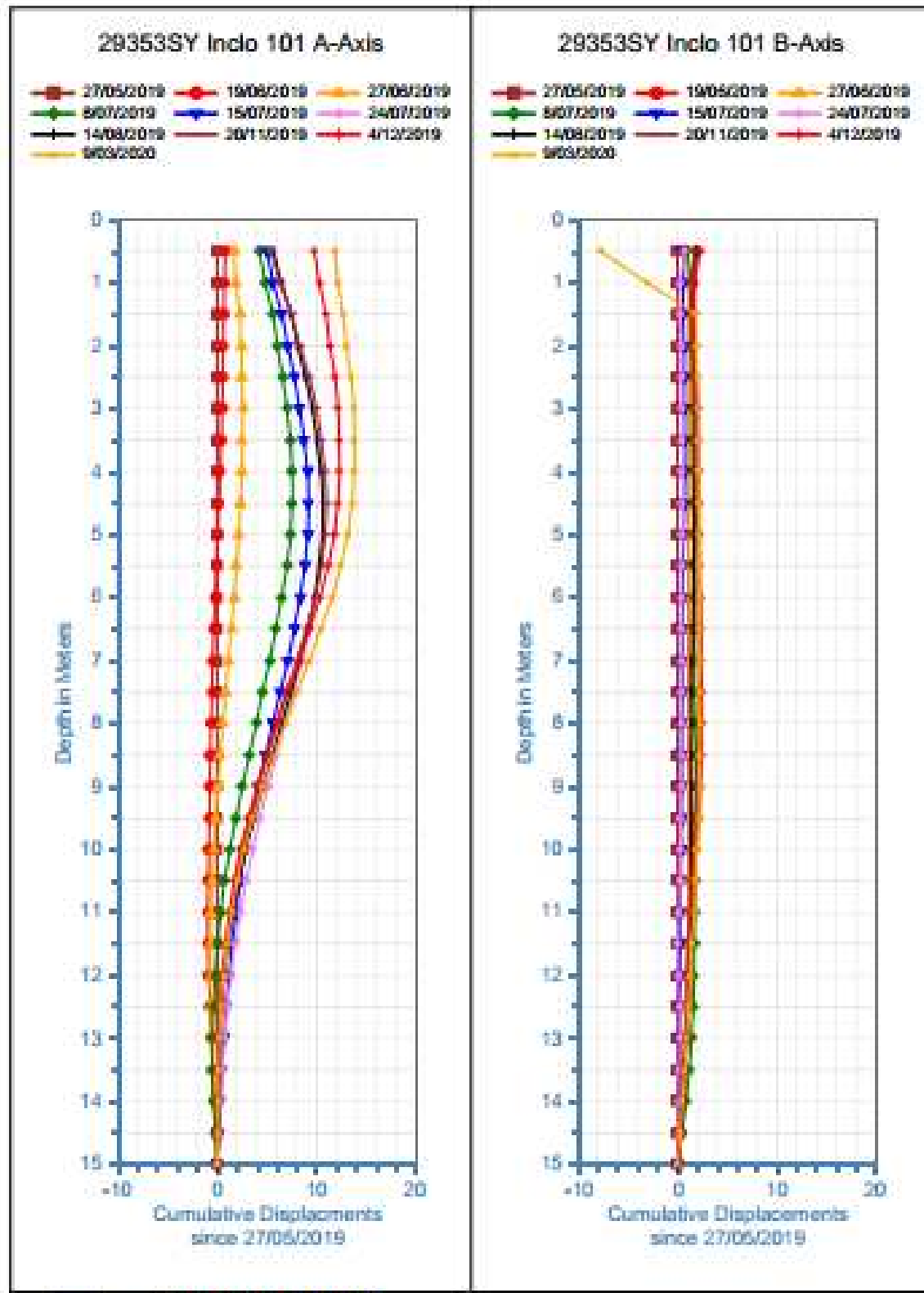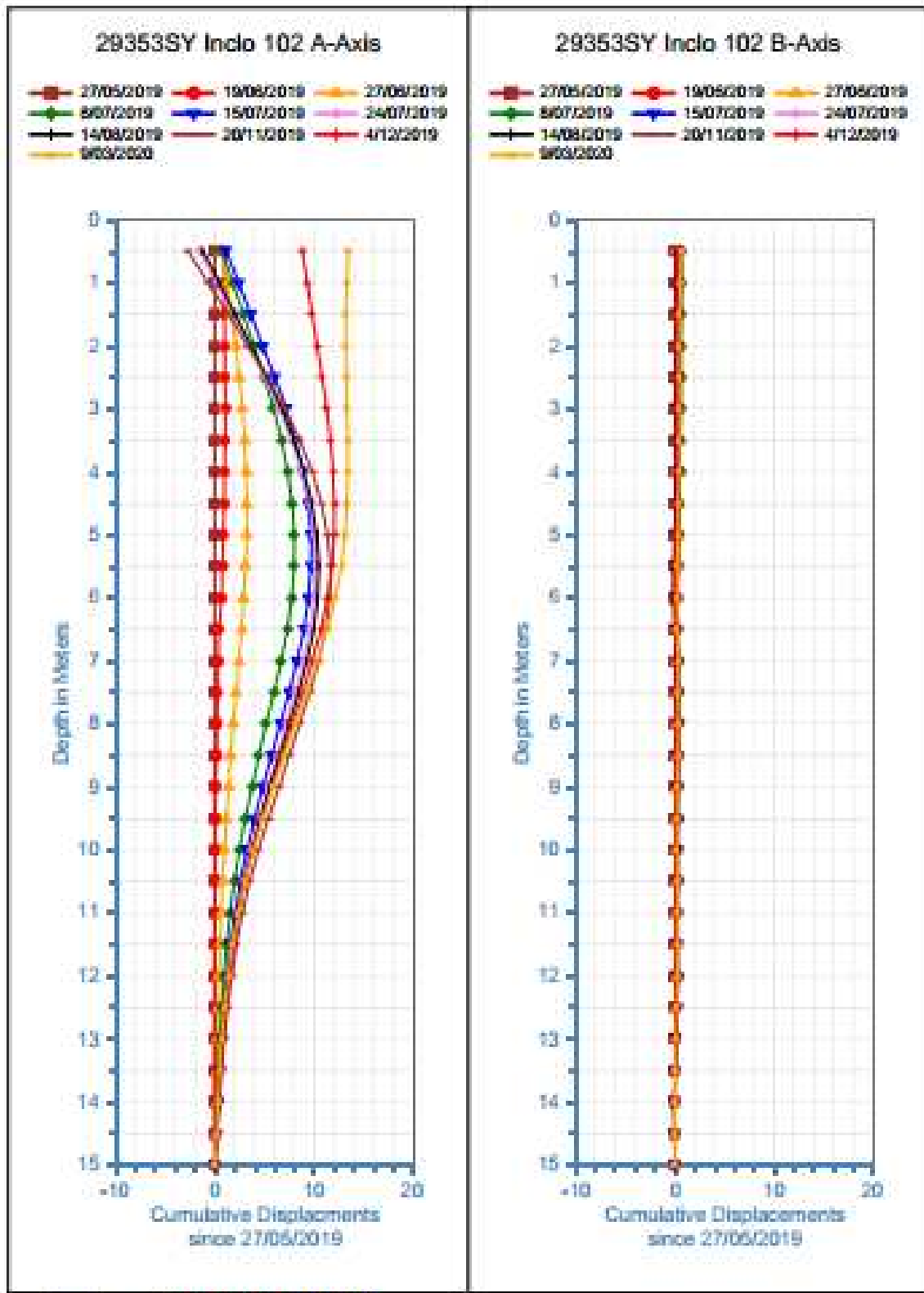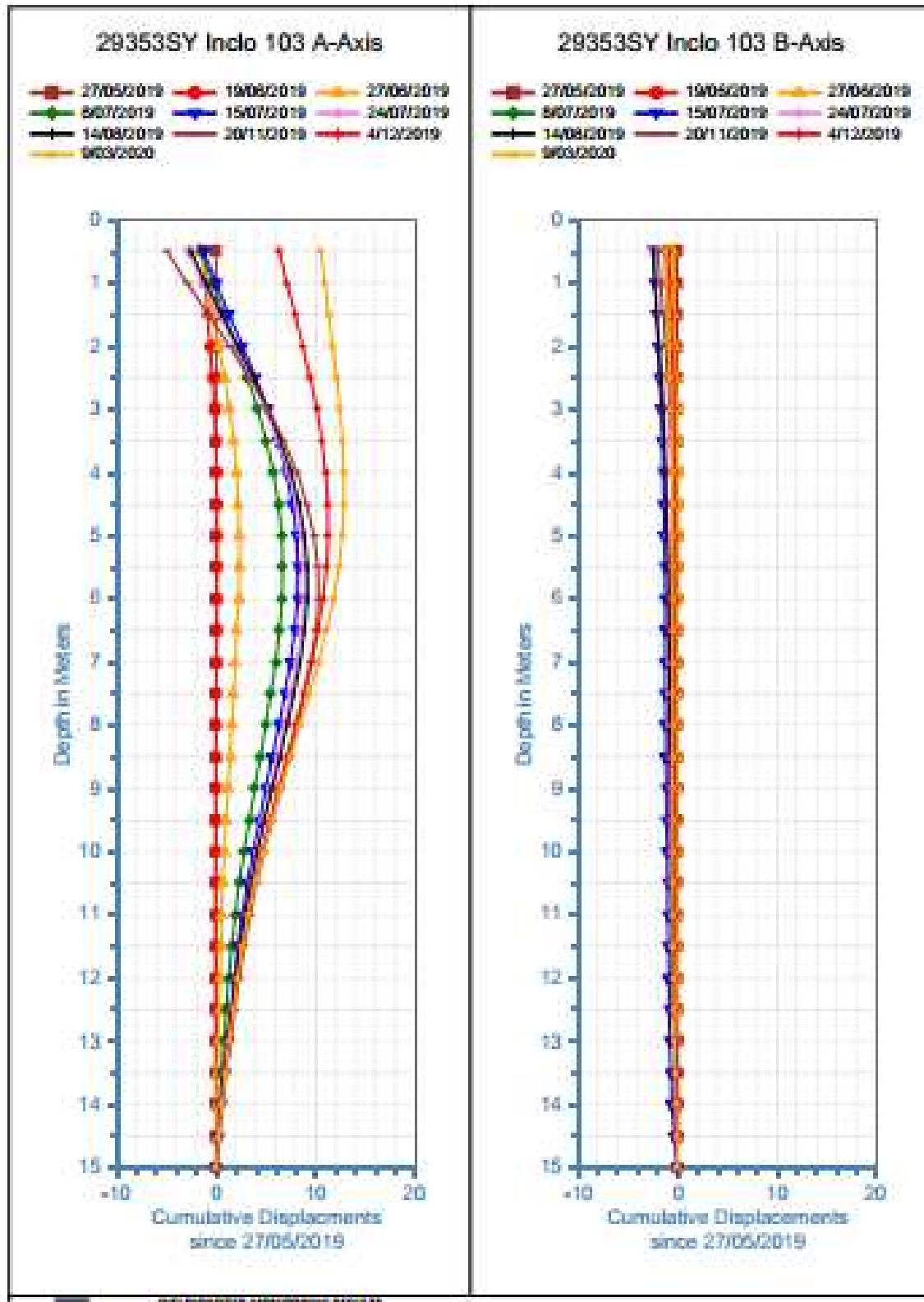
Figure 9. Inclinometer 101.

Figure 10. Inclinometer 102.
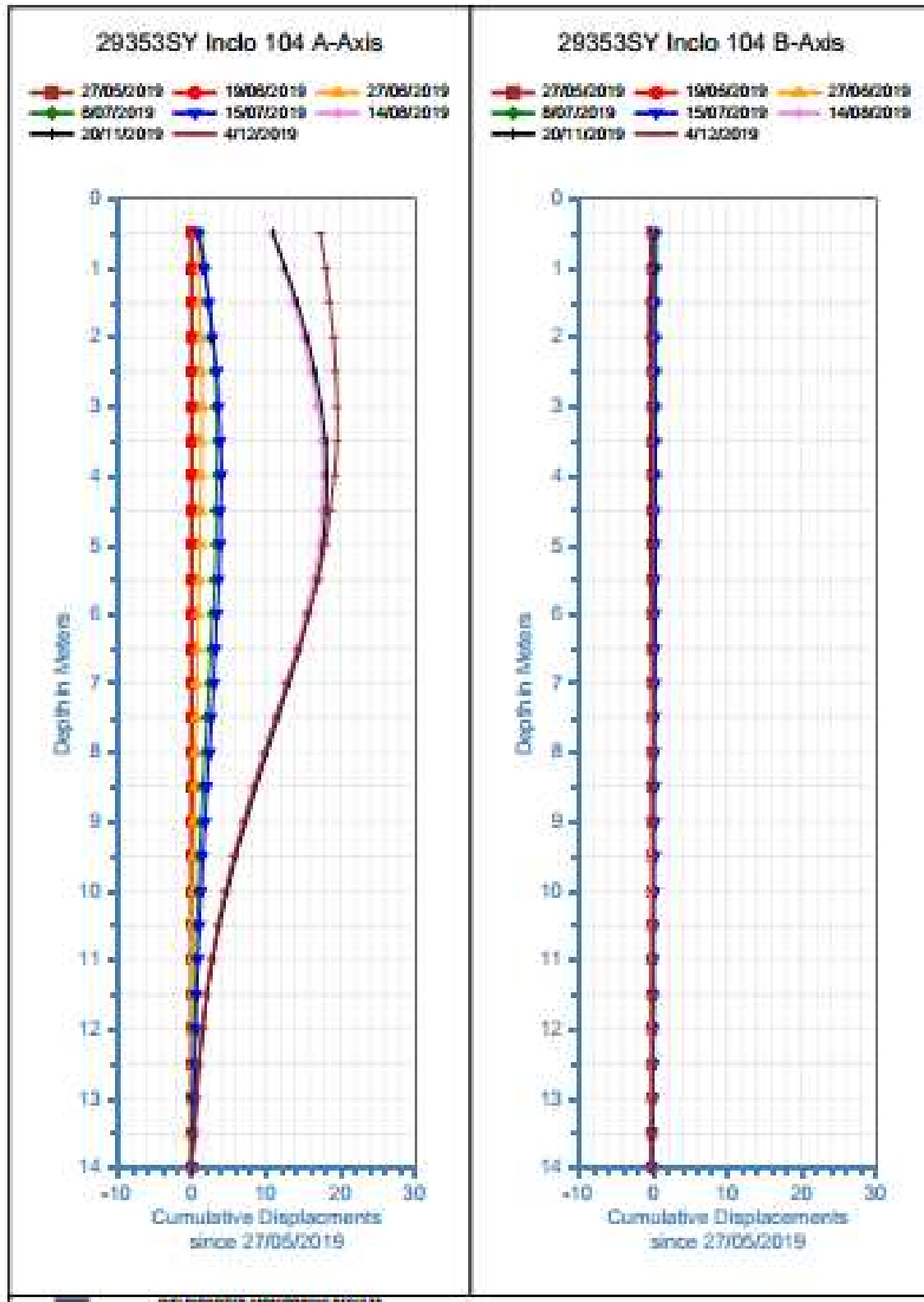
Figure 11. Inclinometer 103.
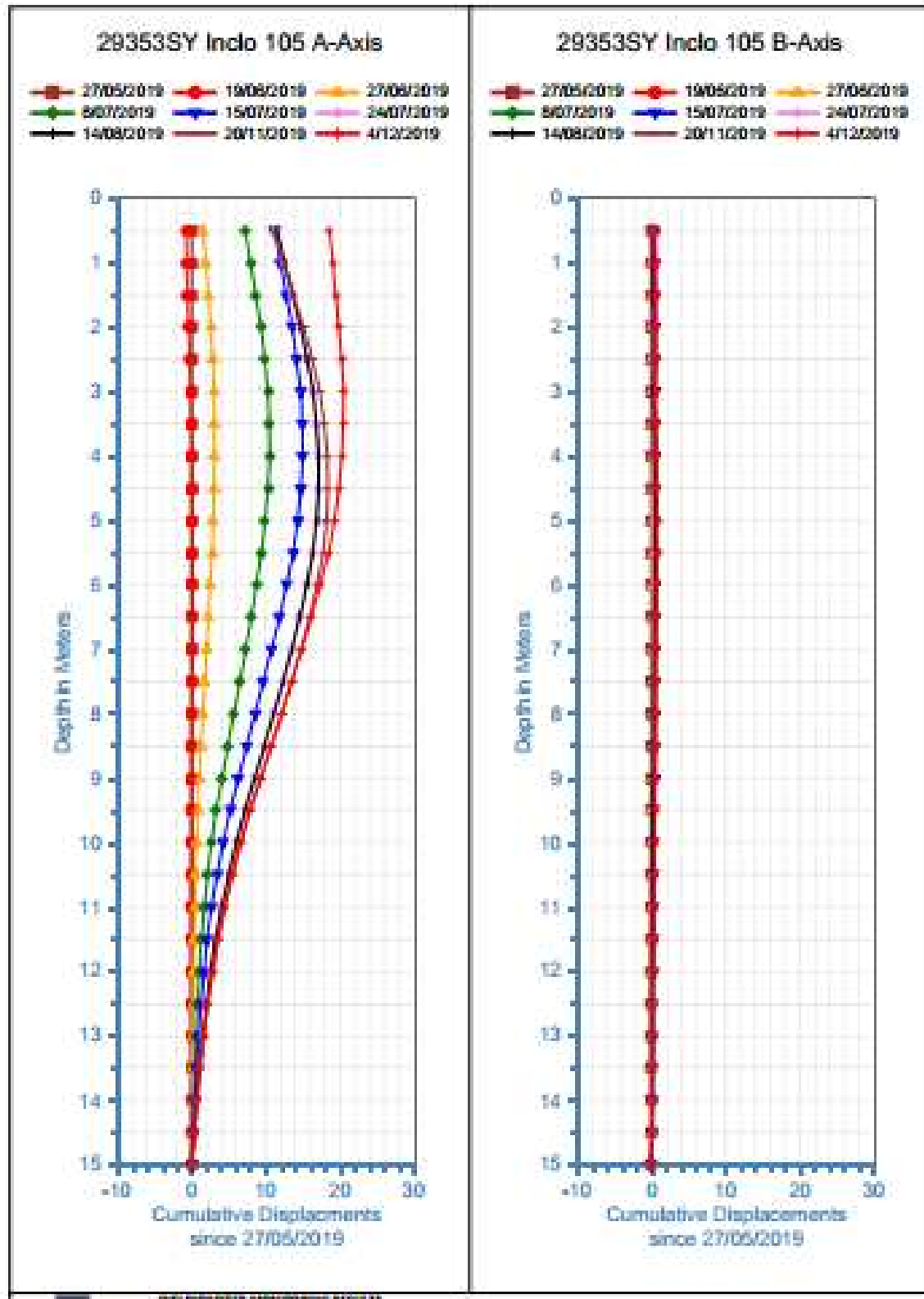
Figure 12. Inclinometer 104.
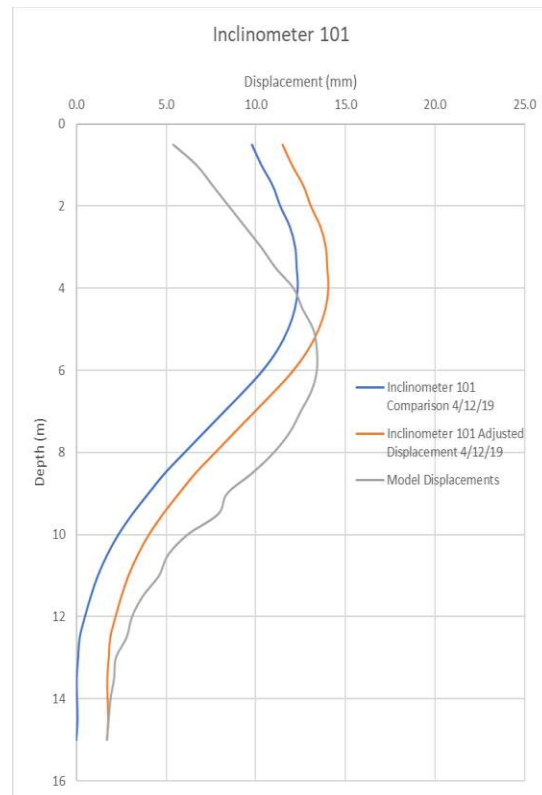
Figure 13. Inclinometer 105.

Figure 14. Inclinometer 101: Comparison of actual and adjusted inclinometer results and predicted movements.
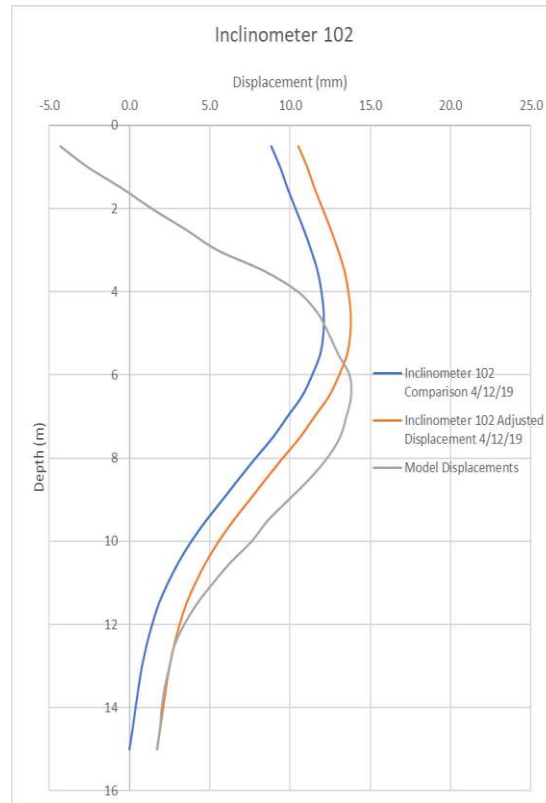

Figure 15. Inclinometer 102: Comparison of actual and adjusted inclinometer results and predicted movements.
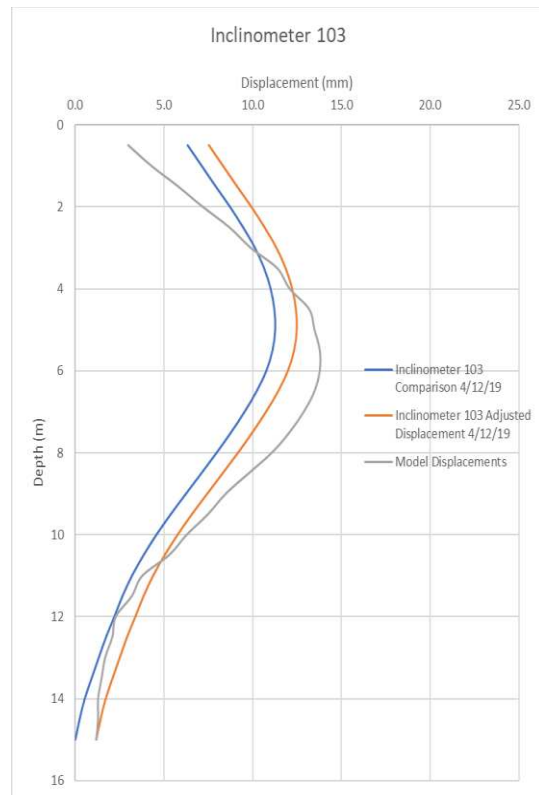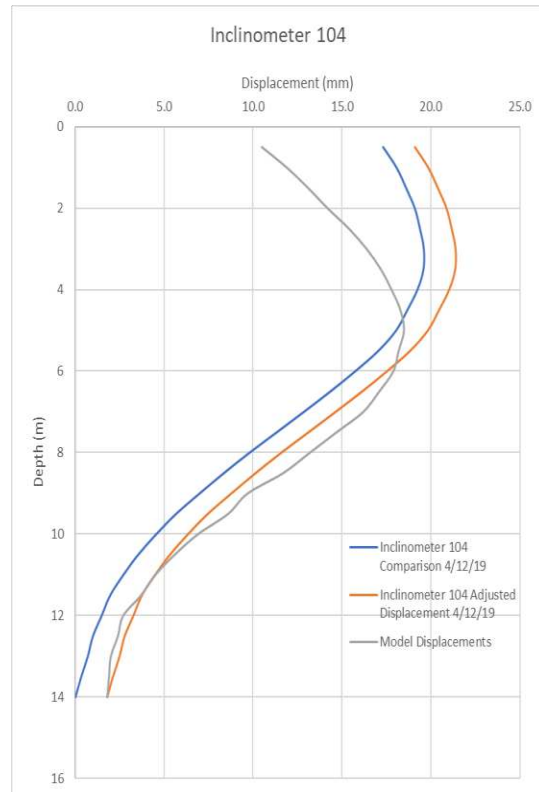
Figure 16. Inclinometer 103: Comparison of actual and adjusted inclinometer results and predicted movements.

Figure 17. Inclinometer 104: Comparison of actual and adjusted inclinometer results and predicted movements.
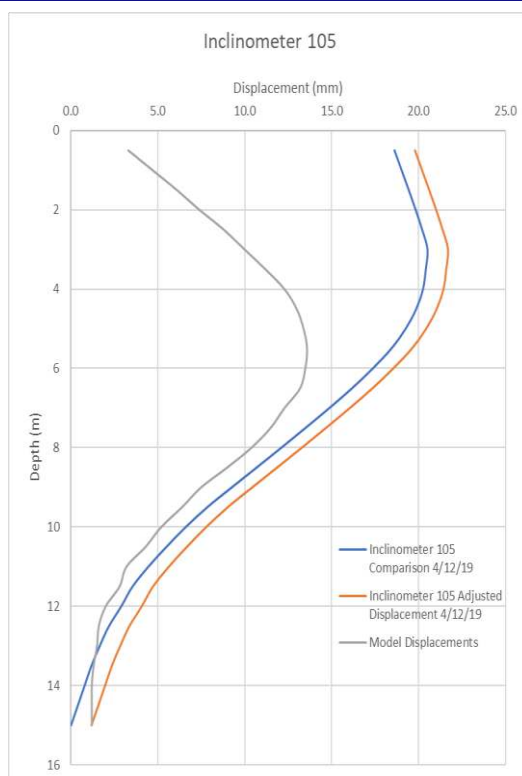
Figure 18. Inclinometer 105: Comparison of actual and adjusted inclinometer results and predicted movements.

As can be seen from the above plots, with the exception of Inclinometer 105, the maximum predicted displacements correlated well with the measured values, with the difference between the predicted and measured displacements at Inclinometers 101 to 103 less than 1.1 mm and at Inclinometer 104 about 3.1 mm. At Inclinometer 105, the model underestimated the actual maximum displacement by about 8 mm.

While the predicted maximum deflections correlate reasonably well with those that were measured, the depth of predicted and measured maximum deflection did not correlate so well. In all cases, the point of maximum deflection is appreciably lower than the point at which it occurred. This appears to be the result of larger predicted inwards (i.e., into the face) deflections at the crest of the wall following jacking of the props. These larger inwards movements result in the inflection point of the wall moving lower. Therefore, the depth of inflection of the wall is lower than it would be if the predicted top of wall displacements were less and more in line with those measured.

Inclinometer Sensibility Check

To improve the predicted displacements to better match the measured movements, the model was re-examined for possible explanations of the observed differences. To this end, a review of the investigation data and the assumptions made during the development of the geotechnical model was completed. In this regard, it was noted that the investigation indicated that in the upper 2.5 m of the subsurface profile, there was variation between test locations in the modulus of the sand. While CPT2 and DMT203 indicated a denser band, CPT3 did not (refer to Figures 4 and 5). Unfortunately, the original purpose of the investigation had been the design of a raft slab; consequently, only one of the three DMT's included testing over the upper 6 m. As a result, a conservative approach was adopted, and the upper unit of soil was assumed to uniformly comprise a very loose sand with a modulus of 20 MPa.

Re-examining the available information suggested that the original assumption may not have been as conservative as was first assumed. Reference to CPT2 and DMT203 suggested that the upper 2.5 m of sand across the site may be typically denser than that modeled. Rerunning the model with the upper 2 m of the profile modeled as loose (i.e., E=50 MPa) rather than very loose sand (i.e., E=20 MPa) changed the predicted deflection of the walls, both in terms of the maximum deflection and the depth at which this deflection occurs. The greatest impact of this change was at the top of the wall, where wall deflections into the face were between about 2 mm to 4 mm smaller than previously predicted. This in turn resulted in the modeling

results better predicting the measured deflections, although the model still underestimated displacements at the top of the wall. Figures 19 to 23 show the change in predicted wall deflections where a denser sand layer was present over the upper 2 m of the model.

While the predicted displacements (with the exception of Inclinometer 103) still did not match the measured movements even after including the loose sand band over the upper 2 m, at the location of Inclinometer 105 the difference between predicted and measured displacements was significantly greater than at other locations. Behind this wall, building materials were periodically stockpiled. Thus, to understand the potential impact of a surcharge load behind the wall, the model was adjusted to include a 10 kPa surcharge applied directly behind the wall at the bulk excavation stage (Stage 5). This resulted in an additional 7 mm of movement at the top of the wall which, when combined with the additional displacements from the upper 2 m being modeled as loose sand, achieved an additional total displacement of 8.7 mm. Notwithstanding this, the predicted displacements still underestimated the measured wall displacements by 6 mm to 8 mm.

Another potential reason for the observed difference between the predicted and measured displacements is if the inclinometer locations, as shown on the plan, are marginally wrong. This would then mean that when extracting data from the model, the predicted displacements would not correlate with the location at which the measurements were taken. To assess whether this may explain the observed difference, we reviewed the predicted lateral displacements of the wall on either side of the inclinometer locations as shown on the plan. This indicated that whilst shifting the inclinometer location slightly would generally increase the predicted displacements and therefore result in a better correlation between the predicted and measured displacements, it did not explain the observed differences.

There is unlikely to be a single cause or element contributing to the observed differences between the modeled and actual displacements; rather, it's likely to be a combination of contributary causes. These may comprise a mischaracterization of the material parameters over portions of the model, extraction of data from the model at sections that do not perfectly align with the location of the measured displacements, construction related causes such as the incorrect jacking sequence and lock off forces of the props, the placement of stockpiles behind the wall, and structural impacts such as shrinkage of structural elements connected to the walls. While we have been unable to identify the cause or combination of the causes of these differences, their magnitudes are very small; for all practical purposes, the model provides a good representation of the physical performance of the structure.
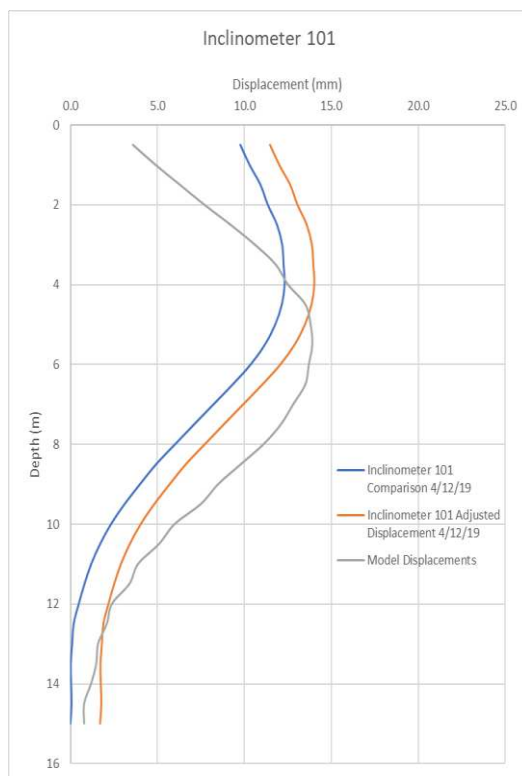

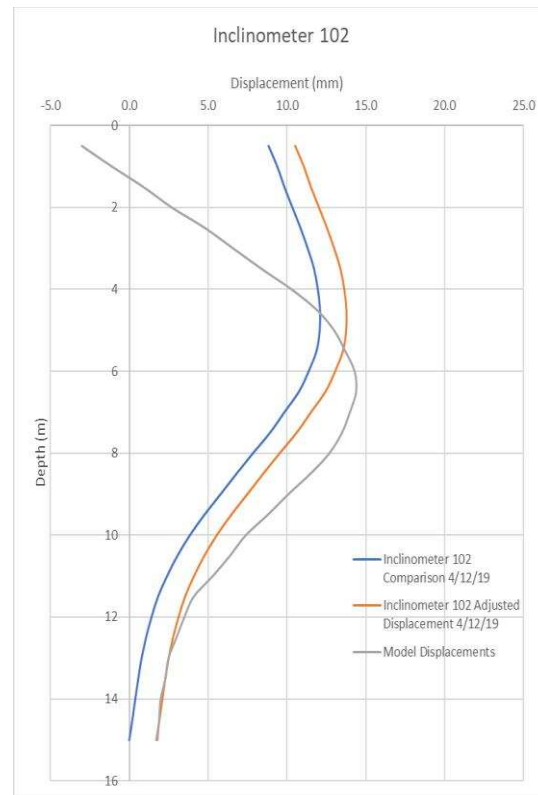Figure 19 - Inclinometer 101 Comparison of actual and adjusted inclinometer results and predicted movements.

Figure 20 - Inclinometer 102 Comparison of actual and adjusted inclinometer results and predicted movements.
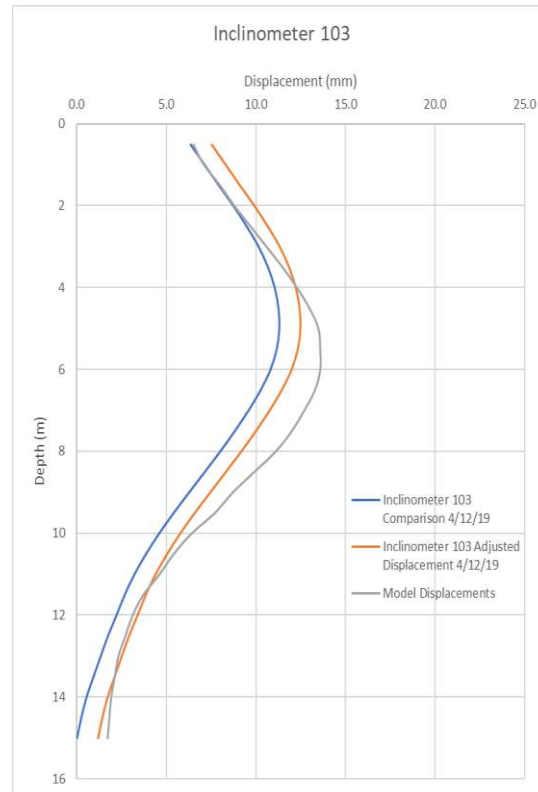

Figure 21 - Inclinometer 103 Comparison of actual and adjusted inclinometer results and predicted movements.
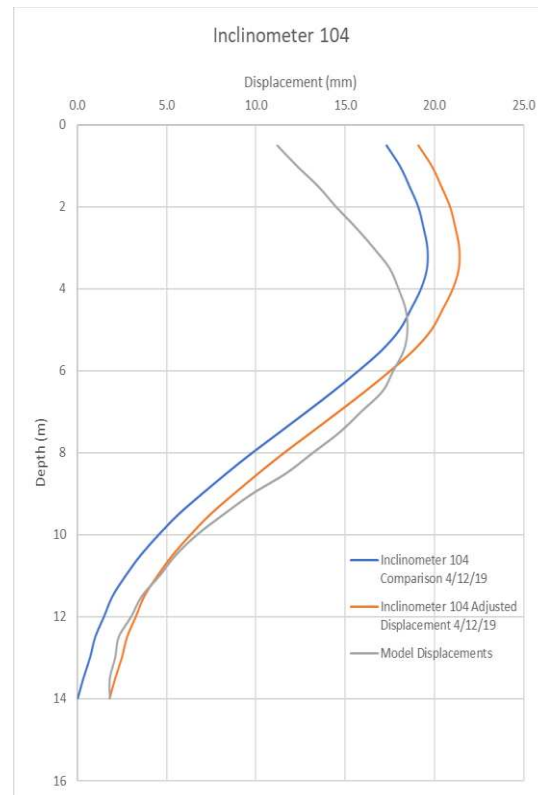
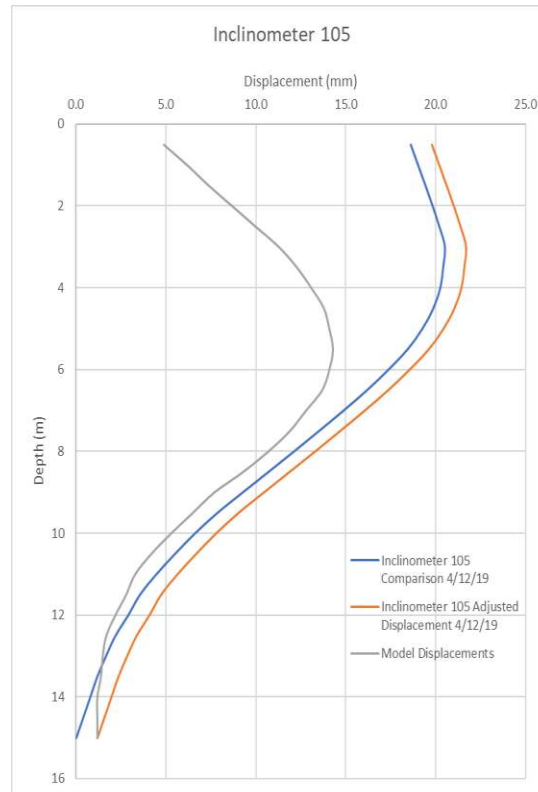*Figure 22. Inclinometer 104: Comparison of actual and adjusted inclinometer results and predicted movements.*

Figure 23. Inclinometer 105: Comparison of actual and adjusted inclinometer results and predicted movements.

Empirical Method Comparison

Previous assessment of the monitoring data from propped excavations *(Li, Li and Tang 2015)* indicated that for a plane strain case (i.e., the length of the wall is sufficient not to be impacted by 3D effects), the ratio between the depth from the ground surface to maximum wall deflection (h_{hm}) normalized by the excavation depth (H) varies from 0.5 to 0.9. Based on the monitoring results, a relationship of 0.69 to 0.82 is calculated, which falls within the relationship range; we note that following removal of the props, however, the depth to maximum deflection shifts up the wall as expected. Furthermore, *Li, Li and Tang* indicated that the relationship between the maximum wall deflection (δ_{hm}) and excavation depth (D) ranges between 0.08% and 0.32% with a mean of 0.16%. While *Wong et al (1997)* suggested the relationship between maximum wall deflection and excavation depth had an average value of 0.2% and a maximum of 0.35%, *Clough and O'Rourke (1990)* and *Ou et al (1993)* suggested that this ratio varies from about 0.2% to 0.5%. Based on the results of our monitoring, this relationship ranged between 0.22% and 0.33%, which showed good agreement with the results of the above papers.

Whilst the results showed good agreement, they were towards the upper end of the reported range of the results reported by both *Li, Li and Tang* and *Ou et al*. In *Li, Li and Tang's* paper, the monitored excavations varied in depth between 15.9 m to 25.3 m and were braced with three to six rows of props. Consequently, it is not surprising that for a 6.5 m deep excavation supported with one row of props positioned at the top of the wall, the ratio of maximum deflection to depth of excavation plots towards the upper end of the range detailed by *Li, Li and Tang*.

Survey Monitoring

Survey monitoring of the capping beam was completed at four locations during construction. The survey monitoring locations are shown in Figure 24 below. Unfortunately, the survey monitoring point on Wall 3 was destroyed sometime after Stage 6.
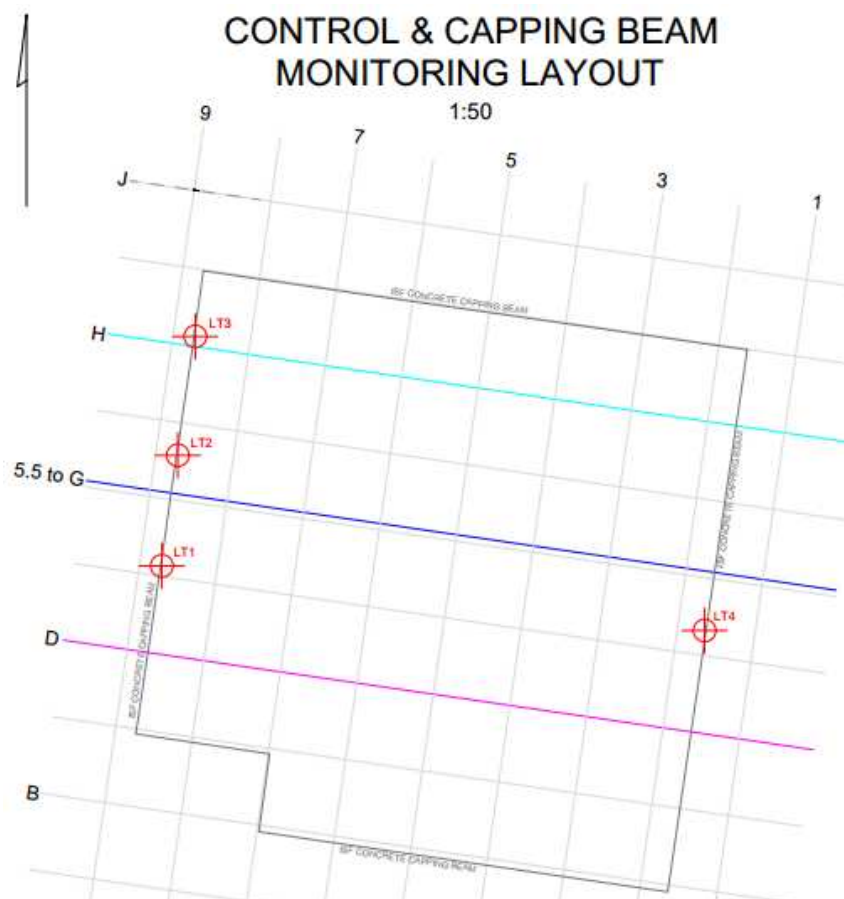

Figure 24. Location of survey monitoring targets.

Table 11 below summarizes the measured displacements at the four survey points along the capping beam, and compares these with the values predicted in our model.

Table 11. Survey Monitoring Results of the Capping Beam Compared with Predicted Displacements.

Monitoring Stage*	CSM Wall	Measured Horizontal Displacement (mm)**	Predicted Displacement (mm)
Stage 4	Wall 1	-6 to -8	-2.7 to -9.4
	Wall 3	-3	-2.0
Stage 5	Wall 1	-2 to 7	-0.1 to -12.4
	Wall 3	19	1.4
Stage 11	Wall 1	11 to 14	-6.1 to 2.2
	Wall 3	N/A	

* The monitoring stage refers to the equivalent monitoring stage for the modeling. It should also be noted that the table only includes the relevant monitoring stages for comparison to the modeling results; additional monitoring was carried out.
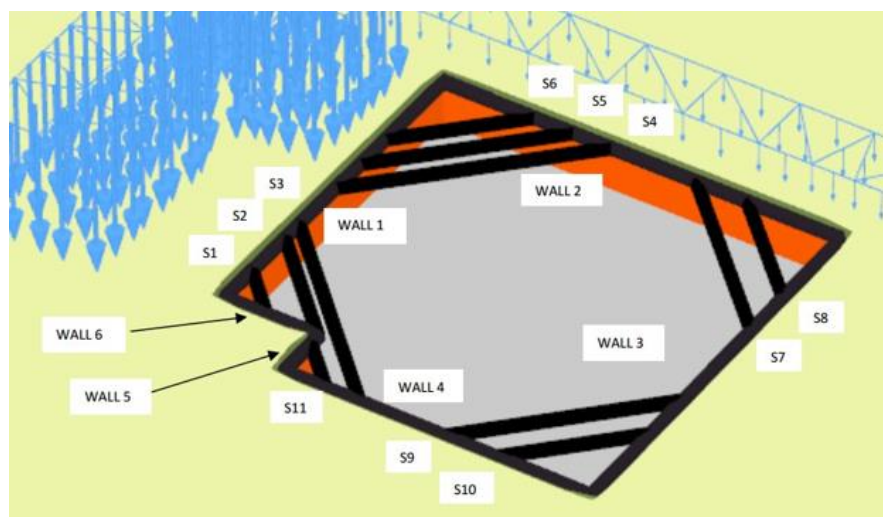** Horizontal displacement perpendicular to the wall. Positive values indicate movement towards the basement excavation.

The survey monitoring results were typically in good agreement with the inclinometer test results. However, it should be noted that while the survey points were specified to be located at the inclinometer locations, while they were located in the vicinity of the inclinometers they were not installed at the same point. Consequently, some difference in results is expected, particularly given the effect of the jacked props on the capping beam.

Monitoring of Forces in Props S3, S4, and S8

Monitoring of the forces in three props, S3, S4, and S8 was completed while the props were in place. The location of these props is shown in Figure 25. Prop forces at various stages in construction were estimated in our numerical analysis. The nominated prestress forces and the predicted forces for props S3, S4, and S8 are shown below in Tables 12, 13, and 14.

The results of the monitoring of the props are shown in graphical form below in Figures 26 to 35. For each prop, the measured forces for each of the critical stages are presented below (i.e., Stage 4 to Stage 5, Stage 6 to Stage 8, and Stage 9 to Stage 10). Tables 12, 13, and 14 present the design, predicted and measured prestress load, and prop forces.
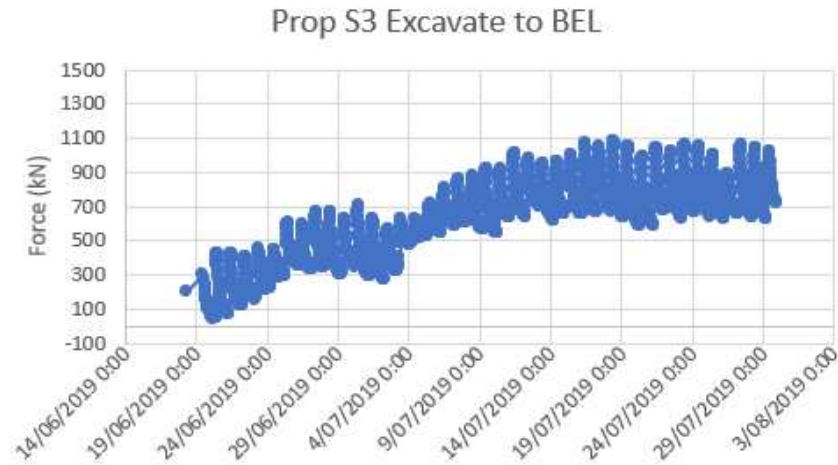

Figure 25. Identification of props.
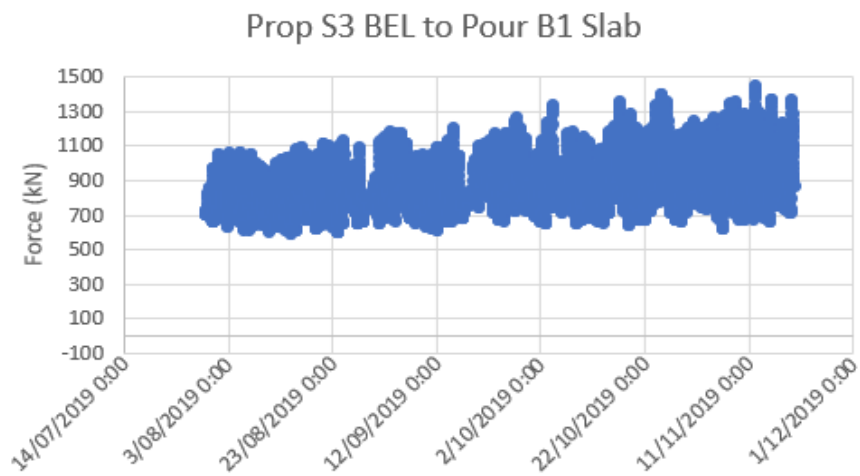
Figure 26. Prop S3 Stage 4 to Stage 5.

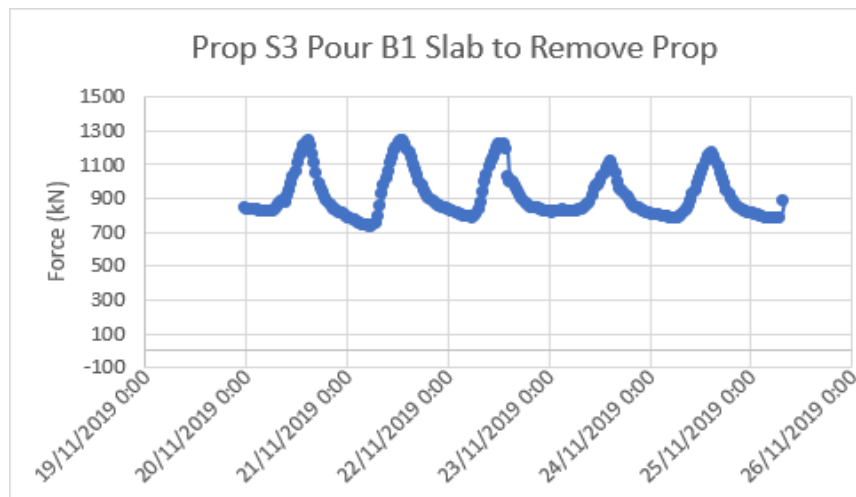
Figure 27. Prop S3 Stage 6 to Stage 8.
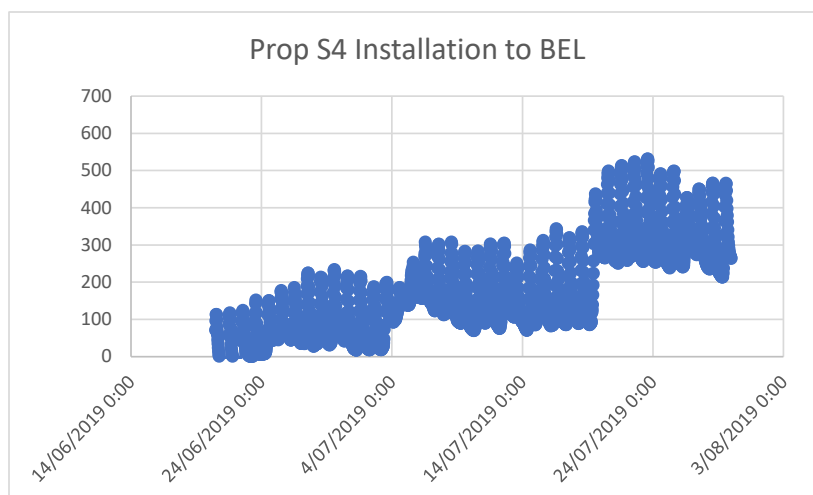

Figure 28. Prop S3 Stage 9 to Stage 10.

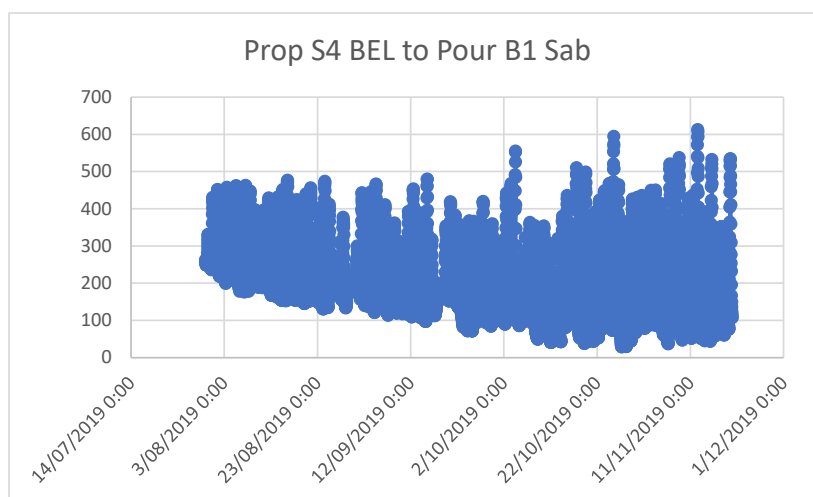*Figure 29. Prop S4 Stage 4 to Stage 5.*

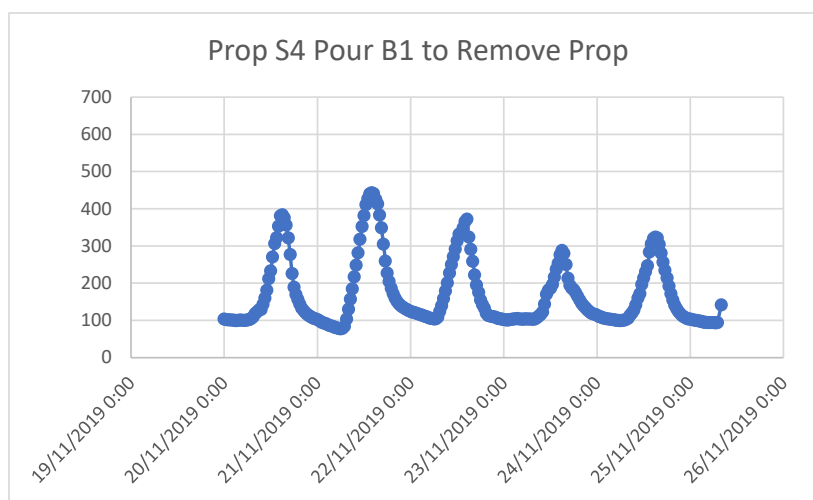
Figure 30. Prop S4 Stage 6 to Stage 8.

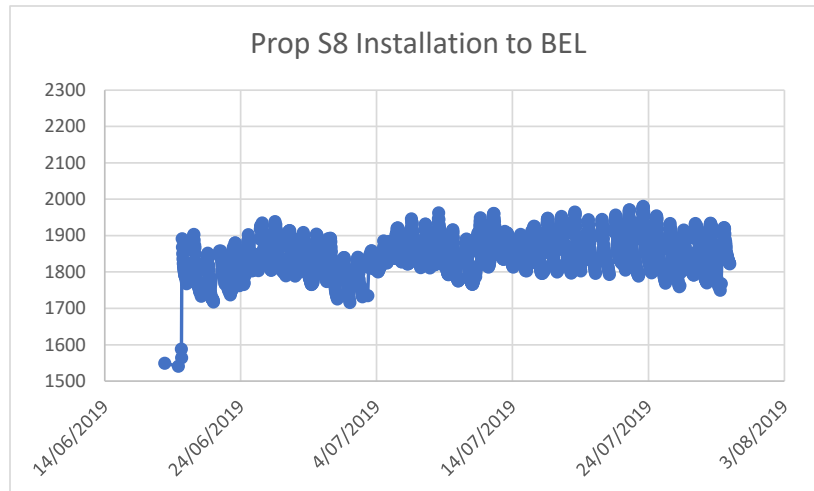*Figure 31. Prop S4 Stage 9 to Stage 10.*
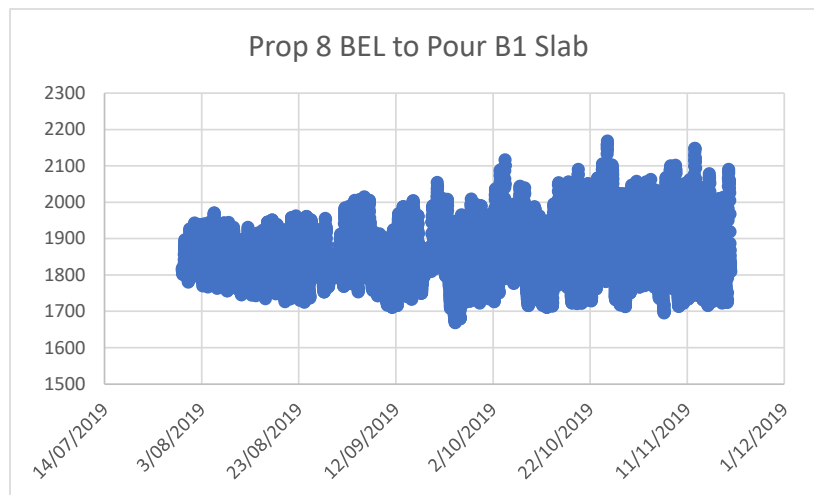
Figure 32. Prop S8 Stage 4 to Stage 5.

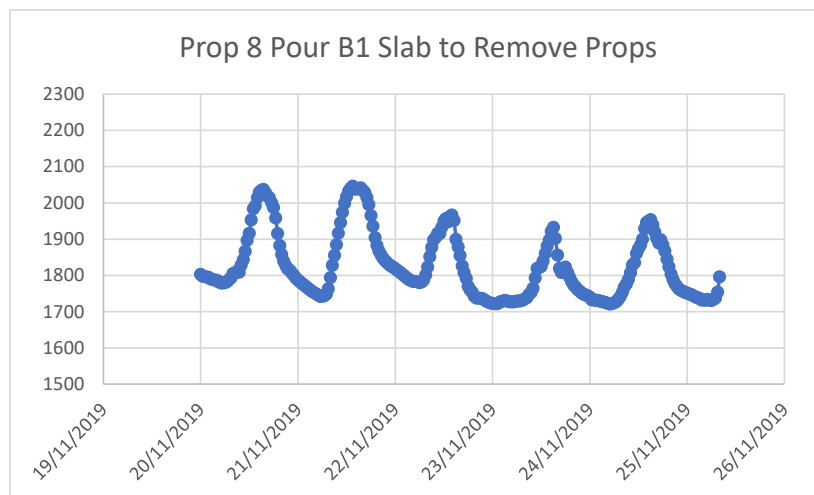*Figure 33. Prop S8 Stage 6 to Stage 8.*

Figure 34. Prop S8 Stage 9 to Stage 10.

Table 12. Prop S3 - Comparison of Predicted and Measured Forces.

	Prestress Load (kN)	Stage 5 BEL to RL-4.7m (kN)	Stage 8 Apply 20% of Column loads to Raft Slab (kN)	Stage 10 Apply 40% of Column loads to Raft Slab (kN)
Design	0	1009	911	936
Measured	200	1084	1424	1242
Difference (%)		7.4	56.3	32.7

Table 13. Prop S4 - Comparison of Predicted and Measured Forces.

	Prestress Load (kN)	Stage 5 BEL to RL-4.7m (kN)	Stage 8 Apply 20% of Column loads to Raft Slab (kN)	Stage 10 Apply 40% of Column loads to Raft Slab (kN)
Design	50	1036	1098	1134
Measured	69	531	613	444
Difference (%)		-48.7	-44.2	-60.8

Table 14. Prop S8 - Comparison of Predicted and Measured Forces.

	Prestress Load (kN)	Stage 5 BEL to RL-4.7m (kN)	Stage 8 Apply 20% of Column loads to Raft Slab (kN)	Stage 10 Apply 40% of Column loads to Raft Slab (kN)
Design	1800	2168	2192	2207
Measured	1850	1980	2168	2046
Difference (%)		-8.7	-1.1	-7.3

The results show S3 was loaded to the wrong prestress load and, as a result, the loads in this prop were significantly higher than predicted (over 50% greater). This also resulted in a reduction in the measured load in S4 when compared to the predicted load. It is likely that the load carried in S2 was also lower than that predicted, although monitoring of this prop was not undertaken. However, upon review of the model, the impact of this increased prestress load in S3 on both the wall movements and forces in the props was not adverse. This highlights the significant interdependency between prop loads and the need to carefully ensure that the design prestress loads are the actual prestress loads applied.

The impact of temperature can clearly be seen with the diurnal change in force, apparent in the above figures. The change in temperature resulted in fluctuations in prop loads of up to about 850 kN. This corresponded to changes in potential wall movements of up to about 2 mm, which allowed for the lengthening in the props due to increase in temperature and elastic shortening for the prop as a result of the increase in load. This also assumes that at the center point of the prop, no movement occurs. While changes in wall movements as a result of changes in temperature are relatively small and are unlikely to have a significant impact on movement sensitive structures behind the wall, an appreciable change in force in the props does occur, which also results in a significant change in internal structural actions within the wall itself. Consequently, the potential increase in load in both the props and the shoring system must be carefully considered in the design of the retention system.

Sensitivity Analysis of Geotechnical Parameters

The selection of the soil parameters and development of the design was an iterative process. An initial model was run using soil parameters that were considered reasonable, derived from the SPT and CPT results. These results were then provided to the structural engineer for review, who then indicated that the magnitude of displacements was excessive. Based on the testing completed, it was not possible to justify a further refinement of the soil parameters adopted; consequently, DMT was

undertaken to justify the adoption of higher parameters. Through the incremental refinement of soil parameters and the design, the magnitude of displacements was reduced to an acceptable level. Still, this process resulted in very little allowance for conservatism in the soil parameters adopted. Consequently, a sound understanding of the potential implications our assumptions could have on the modeling results—and thus the actual performance of the structure—was necessary.

To this end, a sensitivity analysis was undertaken in the design phase of the project to gain an understanding of the potential impact of our ground model assumptions. In terms of wall deflections, the parameters of the sands had the greatest impact. Consequently, lower bound modulus values were adopted over these sand units to see which, if any, had the greatest impact. Tables 15 and 16 below summarize the modulus values originally adopted in the model, those adopted for the sensitivity analysis, and the impact on predicted wall movements for CSM Walls 1 and 3.

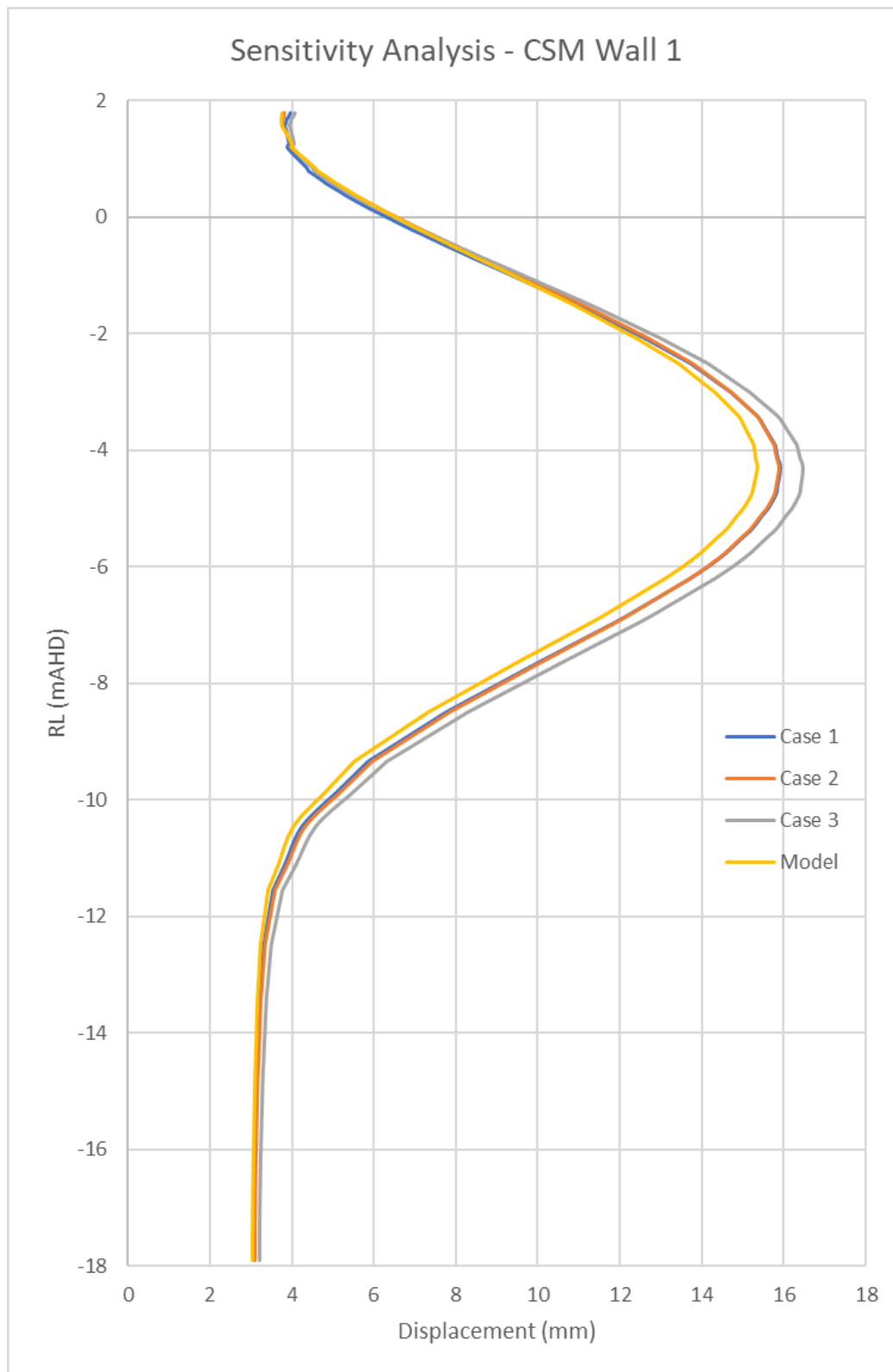*Table 15. Sensitivity Analysis Cases of CSM Wall 1 at Stage 14.*

Sensitivity Case	Design Modulus (MPa)	Maximum Displacement (mm)	Sensitivity Modulus (MPa)	Maximum Displacement (mm)	Difference (mm / %)
Case 1 *Very Loose*	20	15.4	10	16.3	0.9 / 5.8%
Case 2 *Loose* *Dense to Very Dense*	50 161	15.4	45 140	16.3	0.9 / 5.8%
Case 3 *All units reduced*	As above	15.4	As above	17.1	1.7 / 11.0%

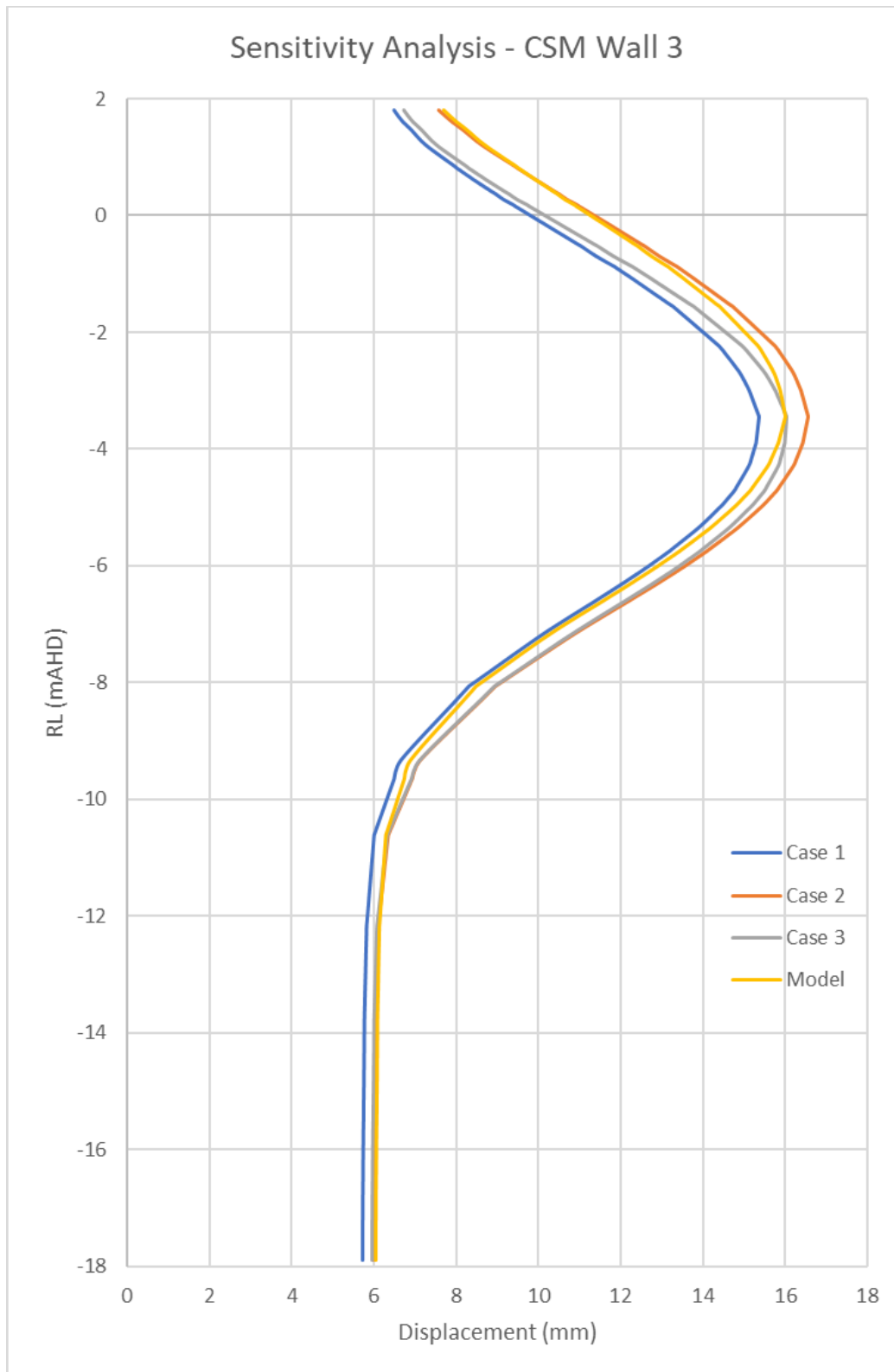*Table 16. Sensitivity Analysis Cases of CSM Wall 3 at Stage 14.*

Sensitivity Case	Design Modulus (MPa)	Maximum Displacement (mm)	Sensitivity Modulus (MPa)	Maximum Displacement (mm)	Difference (mm / %)
Case 1 *Very Loose*	20	16.0	10	15.4	-0.6 / -3.8%
Case 2 *Loose* *Dense to Very Dense*	50 161	16.0	45 140	16.6	0.6 / 3.8%
Case 3 *All units reduced*	As above	16.0	As above	16.1	0.1 / 0.6%

Figures 35 and 36 present plots of the wall displacements at the critical section for the adopted model. These plots represent predicted displacements of Walls 1 and 3 at Stage 14, and include both the results from our design model and the three sensitivity cases considered.

The results indicated that only a nominal change in the magnitude of wall displacements (less than 1.7 mm) occurred when lower modulus values were adopted. For CSM Wall 1, a reduction in the modulus resulted in uniformly greater displacements for all of the three cases considered, with the greatest displacements occurring when the modulus of all the sand units was reduced. Conversely, for CSM Wall 3, a change of modulus had varying results for each sensitivity case. Case 1 resulted in a reduction in the maximum displacement, due to the reduced resistance provided by the soils and the increased deflection at the top of the wall when jacking loads were applied. However, in cases 2 and 3, displacements were either similar or slightly greater than the design model results but the observed impact was overall nominal.

Figure 35. Sensitivity analysis of CSM Wall 1.

Figure 36. Sensitivity analysis of CSM Wall 3.

The sensitivity analysis indicated that while a change in modulus value has different impacts on the walls due to the various structural elements and their interaction, the change in the magnitude of wall deflection was small. Subsequently, the above results suggest that the model was not overly sensitive to minor variations in the modulus values or a large change in the modulus to units of relatively thin layer thicknesses, as discussed above in *Comparisons of Monitoring Results with Predicted Displacements and Forces*, where more than doubling of the modulus of the very loose sand resulted in only a nominal difference in the predicted wall displacements. This provided confidence that minor mischaracterization of the subsurface conditions was not going to result in significant changes for the predicted displacements or the structural actions. Sensitivity analyses were not carried out on the adopted strength parameters (e.g., cohesion, etc.) since the adopted parameters were relatively conservative and few plastic points were observed in the model.

CHALLENGES AND LESSONS

The subsurface conditions across the site posed several challenges. Whilst conventional piled footings to rock with multiple rows of props or anchors could have been adopted to successfully develop the site, such an approach made the project unviable from a financial perspective. Consequently, the challenge was to develop a more efficient design that was financially viable.

To do this, the key, from a geotechnical perspective, was to optimize the geotechnical parameters used in the design. In this regard, the accuracy of subsurface testing, particularly with respect to the modulus values, needed to be improved. This resulted in an iterative investigation approach that progressed from boreholes to CPT's and culminated in the completion of a number of DMT's. The DMT results allowed the justification of higher modulus values than would otherwise be adopted where correlations from CPT results were used. However, as the investigation at this stage was targeted at confirming the viability of a raft or piled raft slab, testing was targeted at depths of greater than 6 m, with only one of the three DMT's tests recording data within the upper 6 m of the soil profile. While it is important to design targeted investigations, it is also important to remember that it is difficult to know what information may be required at a later date and to gather as much information as practicable even if it may not appear relevant at the time.

While the DMT's justified the use of higher modulus parameters, it was important to realize that these parameters were realistic values of the stiffness of the soil. In this regard, very little to no conservatism was built into the model and thus these values, and possible variations in these values and their implications needed to be carefully considered by the completion of sensitivity analysis. As the design of the retention system was a collaborative process between the geotechnical and structural engineers, it was essential that the results of our modeling and sensitivity testing were clearly communicated to the structural engineers, so they too appreciated the assumptions made (and their sensitivity) and they could design the structure with sufficient redundancy for those elements where the greatest uncertainty existed.

A key design consideration for the retention system was to limit both the total and differential settlements below the adjoining building to the west. Initially, two rows of props were proposed along this wall. However, from a constructability point of view, it was decided to adopt a single row of props at the capping beam. To accommodate the removal of the second row of props, the stiffness of the CSM wall was increased, resulting in a closer spacing of the steel beams installed in the CSM walls, which in turn resulted in acceptable induced deflections below the adjoining structure. Whilst the expectation was that once the props were removed there would be no additional induced settlement below the adjoining building, it transpired that roughly one quarter of all settlements were induced by the settlement bowl that formed following the loading of the piled raft.

While a good understanding of the model assumptions and the sensitivity of these assumptions was critical for the design of a sufficiently robust retention system, monitoring the performance of the system during construction formed an essential feedback loop to confirm that the model was a good representation of reality. This feedback loop was required at key stages during construction so that, if necessary, changes to the design could be made where monitoring indicated that displacements or forces exceeded those predicted and were likely to become problematic as construction progressed. To ensure that this monitoring system would be operational over the construction period, it was important to build redundancy into it so if the monitoring points were damaged or lost, a functioning system would still exist. In addition, it was also important that, where possible, the monitoring system allowed for a confirmatory check that the monitoring itself was reliable. In this regard, the survey monitoring was completed at the capping beam near the top of the inclinometers. The monitoring provided several insights. These were:

- Where monitoring has limitations (i.e., the toe of the inclinometer was not fixed), the monitoring results need to be corrected to reflect any inherent inaccuracies by comparing with other monitoring methods, e.g. comparing the survey and inclinometer results.

- While DMT's and published correlations *(Marchetti et al. 2001)* have been used for many years, the correlations were based on testing completed on sands in Europe, Japan, and South America, and were not specific to Sydney's marine sands. The results of the monitoring provided confidence that these published correlations are equally valid for marine sand deposits in the Sydney basin.

- That diurnal temperature changes have an appreciable impact on the performance of props. While this impact is not large in terms of deformation, it can be large in terms of force. In this case, there was a force variation of up to 850 kN. This is a significant variation and may provide a substantial change in the forces developed in structural elements. This potential impact must be considered at the design stage so that the structural engineer can appropriately design the structure.

- That good site control is essential to ensure that critical elements, such as jacking and lock off of the props, are completed in accordance with the design.

Although good communication is always significant, it was particularly important that clear communication between the relevant stakeholders (e.g., the builder, structural engineer, contractors, etc.) was maintained at all times due to the collaboration between the geotechnical and structural engineers in the design of the retention system.

CONCLUSION

The numerical modeling and design of a propped CSM retention system was successfully carried out by adopting the following procedures and considerations:

- Accurate characterization and justification of the adopted soil parameters;

- Accurate representation of the proposed structure and construction staging;

- Sensitivity analysis to assess the potential implications of any assumptions made;

- Continuous and clear communication between the geotechnical and structural engineers;

- Monitoring at key stages of the construction to validate the model and assumptions, and to provide an early warning system to allow for the installation of remedial measures should the predicted values not match measured values;

- A monitoring system that included inbuilt redundancy and differing monitoring techniques to verify monitoring results where practicable; and

- Identification of inaccuracies in monitoring and the correction of these results.

The major observations and lessons learned from the results of the numerical analysis and collected monitoring data are summarized below:

- The correlations proposed by *Marchetti et al. 2001* appear suitable for use on Sydney marine sands.

- Soil-structure interactions are complicated due to the limitations inherent in site testing and proving, and it is generally difficult to replicate the inherent subsurface variability. Using the information obtained from the site investigation program, it may not be possible to entirely match the predicted and measured displacements/forces or capture all contributing causes of the observed wall performance. Notwithstanding this, it is important to keep in perspective the magnitude of the observed differences and their potential impact.

- Induced settlements below adjoining structures may not end once the temporary support is removed from the walls. Additional settlement may occur as a result of the settlement bowl that extends beyond the footprint of the building once it is loaded.

- Care must be taken that jacking lock off loads match design loads.

- The impact of diurnal temperature changes on the performance of props must be considered at the design stage. Whilst changes in displacements because of diurnal temperature changes were nominal in this case, changes in the load varied up to 850 kN, which had an appreciable impact on the design of the structure.

ACKNOWLEDGMENTS

REFERENCES

Bowles, J. E. (1988). *Foundation Analysis and Design*, 4th Edition, McGraw-Hill.

Clough, G.W., O'Rourke, T.D. (1990). *Construction Induced Movements of an Insitu Wall*, P.C. Lambe, L.A. Hansen (Eds.), Design and performance of earth retaining structures, American Society of Civil Engineers (ASCE), New York (1990), 439-470.

Denver, H. (1982). "Modulus of Elasticity Determined by SPT and CPT." *Proc. of Second European Symposium of Penetration Testing (ESOPT II)*, Amsterdam, Netherlands, Vol. 1, 35-40.

Li, D., Li, Z., and Tang, D. (2015). "Three-dimensional effects on deformation of deep excavations." *Proc. of the Institution of Civil Engineers*, Geotechnical Engineer.

Marchetti, S., Monaco, P., Totani, G., and Calabrese, M. (2001). *The Flat Dilatometer Test (DMT) in Soil Investigations*, A Report by the ISSMGE Committee TC16. Proc. IN SITU 2001, Int. Conf. on in Situ Measurement of Soil Properties, Bali, Indonesia.

Ou, Chang-Yu, Hsieh, Pio-Go, and Chiou, Dar-Chang (1993). "Characteristics of Ground Surface Settlement During Excavation." *Canadian Geotechnical Journal*.

Poulos, H. G. (1988). *Marine Geotechnics*, London: Unwin Hyman.

Schanz, T., Vermeer, P. A., Bonnier, P. G. (2000). *The Hardening Soil Model: Formulation and Verification*, Beyond 2000 in Computational Geomechanics, Rotterdam.

Wong, I.H., Poh, T.Y. and Chuah, H.L. (1997). "Performance of Excavations for Depressed Expressway in Singapore." *Journal of Geotechnical and Geoenvironmental Engineering*, 123 (7), 617-625.

The open access Mission of the International Journal of Geoengineering Case Histories is made possible by the support of the following organizations:

dar al-handasah
shair and partners

Geosyntec
consultants

engineers ı scientists ı innovators

CONETEC

ENGEO
CELEBRATING **50** YEARS
OF ENGINEERING EXCELLENCE

Access the content of the ISSMGE International Journal of Geoengineering Case Histories at:
https://www.geocasehistoriesjournal.org